NACA-TN 4158
C.1

NACA TN 4158

TECH LIBRARY KAFB, NM
0067027

NATIONAL ADVISORY COMMITTEE FOR AERONAUTICS

TECHNICAL NOTE 4158

LOAN COPY: RETURN TO
AFWL (WLIL-2)
KIRTLAND AFB, N MEX

ACCELERATIONS IN TRANSPORT-AIRPLANE CRASHES

By G. Merritt Preston and Gerard J. Pesman

Lewis Flight Propulsion Laboratory
Cleveland, Ohio

Washington
February 1958

TECH LIBRARY KAFB, NM
0067027

NATIONAL ADVISORY COMMITTEE FOR AERONAUTICS

TECHNICAL NOTE 4158

ACCELERATIONS IN TRANSPORT-AIRPLANE CRASHES

By G. Merritt Preston and Gerard J. Pesman

SUMMARY

Full-scale transport airplanes were crashed experimentally to determine the crash loads that result from a variety of crash events. It was concluded that pressurized transport airplanes can withstand high-impact-angle crashes and still maintain survivable areas within the fuselage. During unflared-landing crashes greater fuselage crushing occurred with high-wing than with low-wing airplanes. Airplanes with strong fuselage structures that do not deform and produce sharp, well-supported plowing edges will have relatively low longitudinal acceleration during crashes similar to those studied. Normal accelerations exceeding human tolerance can occur in crashes in which modest fuselage damage occurs. Within the structural range represented by the airplanes crashed, the configuration of the airplane had little effect on the normal acceleration.

INTRODUCTION

Problems of impact survival in airplane crashes have been studied intensively by various research groups. However, full-scale acceleration data have been lacking in this field of study. Such data have now been obtained by the NACA by a series of experimental airplane crashes.

A study of crash-impact survival in light airplanes is reported in references 1 and 2. A similar study for fighter airplanes is reported in reference 3. This report discusses crash-impact survival in transport airplanes.

The data for this investigation were obtained by crashing full-scale airplanes. Three types of transport airplanes were crashed. One type was representative of pressurized low-wing transports. The second represented unpressurized low-wing tranports; and the third, high-wing unpressurized transports. The experimental crashes simulated takeoff and landing accidents that involved fuselage damage ranging from moderate to severe. Landing or takeoff crashes were studied because they occur at low speed where the chance for survival of the impact is high. Accelerations were measured by accelerometers installed on the cabin floor.

The characteristics of the acceleration of the cabin floor during a crash that are important to impact survival are the peak magnitude of the acceleration, the time required for the acceleration to attain peak magnitude, and the time duration and the direction of the acceleration. The data obtained in this study provide information on all of these characteristics.

CRASH PROCEDURE

The procedure used for these experimental crashes is completely described in reference 4. Briefly, the procedure was to guide the unmanned airplanes along a runway under their own power into a set of obstacles designed to produce the desired series of crash events. The airplane was guided by fastening the nose wheel strut or the main wheels to a guide that followed a steel rail placed in the center of a paved runway. Only enough fuel was supplied to run the engines until the airplane reached the crash site. This prevented a large crash fire.

The crash site was arranged so that the desired sequence of events would result. For example, if an unflared landing was desired, the landing wheels were first torn off by earth and timber abutments (fig. 1(a)). The airplane then flew across a pit and onto the inclined face of an earthen mound (fig. 1(b)). Various angles of impact (angle between the airplane trajectory and ground) could be obtained by changing the angle of the mound's face.

If a groundloop crash was desired, only one of the main landing wheels was torn off. The wing tip on the same side would then fall and drag on the ground. This off-center drag would gradually turn the airplane around. If it was thought the wing-tip drag would not turn the airplane rapidly enough, additional obstacles were placed in the wing's path (fig. 1(c)). By similar means, a variety of landing or takeoff crashes could be simulated.

As the airplane moved across the crash site, high-speed motion pictures of the action were obtained from several directions (fig. 1(d)). Motion pictures were also taken of the events occurring inside the airplane during the crash. These motion pictures were synchronized with each other and with the recorded accelerations by means of a timing system.

The cabin-floor accelerations were recorded by either a telemetering or magnetic-tape system. In all cases, accelerations were measured in directions parallel to the three principal axes of the airplane. These are called longitudinal, lateral, and normal accelerations.

The service-weary airplanes used for this study were provided by the military services. Three types of airplanes were used. The type

representing a pressurized low-wing transport is shown in figure 2(a). This airplane was designed for high-altitude pressurized flight and has the gross structure characteristic of this airplane class. The airplane shown in figure 2(b) is representative of low-wing unpressurized transports. The fuselage belly and undersides of the nacelles are approximately on the same level, so that in crashes in which the airplane strikes the ground while moving in its original direction, such as in an unflared landing, the impact forces will be taken simultaneously by the three surfaces. Since this airplane was not designed for pressurized loads, its structure was quite different from that of the pressurized transport.

The unpressurized high-wing airplane (fig. 2(c)) is a cargo-carrying airplane having an integral floor and belly structure throughout the main fuselage. The nose section of the fuselage, however, is a weaker structure covering the front wheel and strut and also serving as an aerodynamic fairing. The main fuselage structure is suspended from the wing. If the main landing gear fails, however, the fuselage structure must support the entire wing, nacelle, and fuel-tank load.

RESULTS AND DISCUSSION

Accelerations in Horizontal Plane

The variables in a crash that affect the accelerations are the attitude of the airplane during successive impacts, the airplane structure, the velocity of the airplane, and the type of surface or obstacles the airplane hits. These are the factors that a full treatment of crash-impact loads should cover. However, since the number of airplanes available was limited, the effects of impact velocity and the type of surface were not studied. Therefore, only the effects of the impact attitude and the airplane configuration on the crash accelerations in the horizontal plane are discussed. Accelerations normal to the horizontal plane are considered in a subsequent section.

Effect of crash attitude on longitudinal acceleration. - During a crash, an airplane may hit the ground in many ways. The ways that were studied in this investigation are as follows:

(1) The airplane strikes an object or the ground while traveling in a straight path.

(2) The airplane strikes obstacles while moving sideways or backward.

(3) The airplane slides along the ground while rotating around its vertical axis as in a groundloop.

(4) The airplane tumbles and rolls as in a cartwheel crash.

Consider first the type of crash in which the airplane strikes the ground while traveling in its original direction as in an unflared landing. Three low-wing pressurized transport airplanes were crashed at angles of impact of 5°, 15°, and 29° (angle between airplane trajectory and ground). Sequence pictures taken from motion pictures of the initial impact of these airplanes with the ground are shown in figure 3. Following each set of pictures are the acceleration data recorded on the fuselage floor.

In interpreting the acceleration data obtained in this investigation, the high-frequency structural vibrations are ignored, because vibrations of this frequency would undoubtedly be damped out by the seat and its occupant. The faired curves superimposed over the acceleration traces eliminate the high-frequency components.

Because of the large number of acceleration traces obtained in this investigation, the pertinent information has been summarized and is presented in table I. Because of their importance with respect to human tolerance, the maximum acceleration obtained and the time required to reach this maximum are emphasized in reviewing the acceleration data. The duration of an acceleration is also physiologically important. Over wide ranges, variations in the duration of an acceleration can affect the human tolerance markedly. Within the range of durations found in these experimental crashes, however, the human tolerance is not affected significantly; therefore, the variations in pulse duration are not discussed extensively in this report.

The longitudinal accelerations presented in figure 3(a) were measured on the fuselage floor at a station 270 inches from the nose of the pressurized transport during the 5° crash. The impact speed for this crash was 81 miles per hour. A maximum acceleration of only 2.5 g's was reached 0.190 second after nose impact. The pulse lasted about 0.3 second and produced a velocity change of 10 miles per hour.

The accelerations resulting from the first impact of the airplane with the ground in the 15° crash of the pressurized transport (fig. 3(b)) were obtained at four locations on the fuselage floor (250, 360, 485, and 680 in. from the airplane nose). These accelerations endured for about 0.22 second, and the acceleration pulses were approximately sinusoidal in shape. The maximum acceleration measured on the cabin floor varied from 11 to 7 g's, with an average of approximately 9.0 g's (fig. 4(a)). The time at which the maximum acceleration on the floor occurred varied from 0.120 to 0.125 second after nose impact, depending on the location in the airplane. The impact speed of this crash was 93 miles per hour; the initial impact of the airplane with the ground decreased the airplane velocity 28 miles per hour.

In the 29° crash of the pressurized transport (fig. 3(c)), accelerations were also measured at four stations (185, 335, 490, and 685 in. from nose). These accelerations endured for approximately 0.23 second, resulting in a velocity change of 50 miles per hour. The impact speed

for this crash was 97 miles per hour. The maximum accelerations are plotted against airplane station in figure 4(b). The maximum acceleration varied from 22 to 17 g's, the average maximum acceleration being about 20 g's. The time at which these maximum accelerations occurred varied from 0.145 to 0.155 second after nose impact.

In order to compare the accelerations of the various crashes, these recorded data were corrected to a common impact speed of 95 miles per hour by assuming that the maximum acceleration resulting from the first impact of the airplane with the ground varied directly with the initial momentum and thus with the initial velocity. The variation of corrected maximum acceleration with impact angle for the various pressurized transport crashes is shown in figure 5. These data show that the longitudinal acceleration increases with increasing angle of impact. This trend would probably continue up to an impact angle of 90°, or up to the impact angle at which the ultimate crushing strength of the fuselage structure has been reached.

A crash of this type of pressurized airplane at Louisville, Kentucky, permits the data obtained in this investigation to be extrapolated. This airplane crashed at an estimated angle of impact of 50° and an impact velocity of 150 mph. The angle of impact was established by the CAB during its investigation of the accident (ref. 5). The impact speed was determined by flight tests simulating the condition of the crash by Aviation Crash Injury Research of Cornell University. The nose section forward of the wing collapsed completely in this crash, as shown in figure 6. The maximum acceleration resulting from this crash, calculated by assuming the stopping distance shown in figure 7 (from the CAB accident investigation) and also assuming the acceleration pulse to be a half sine wave, is 47 g's. If these data are corrected to 95 miles per hour, the nominal impact speed of the crashes of this investigation, a value of 30 g's is obtained. This data point indicates that the trend shown by the data of figure 5 continues up to an impact angle of 50°. Since the airplane that crashed at Louisville experienced an estimated acceleration of 47 g's in crushing the nose structure back to the leading edge of the wing without destroying the living space aft of the wing, the ultimate crushing strength of the fuselage is at least 47 g's.

The fuselage distortion that resulted from the experimental crashes of this investigation was relatively minor. During the 5° crash the fuselage received practically no damage (fig. 8(a)). The major damage was the ripping off of the engines. The holes in the side of the fuselage were caused by flying propeller blades. Likewise, the damage inflicted on the airplane in the 15° and 29° crashes was minor (figs. 8(b) and (c)). The large holes in the fuselage fore section of the 15° crash (fig. 8(b)) were caused by flying propeller blades. The maximum acceleration of 20 g's in the 29° crash resulted in damage that would not jeopardize the safety of the occupants of the airplane. Even the cockpit was completely

intact. It may be concluded from the amount of crushing that occurred in the 29° crash that the fuselage structure of this airplane is capable of withstanding severe crashes and still maintaining areas in which the structure does not collapse. These areas can be called survival areas.

Effect of crash attitude on horizontal accelerations from side and rear. - The unflared-landing crashes just discussed are not the only type of crashes in which there are large accelerations in the horizontal plane. There has been considerable discussion in the aircraft industry as to whether higher accelerations may be applied from the side or the rear of the airplane in crashes where the airplane turns around during the crash and then strikes an object as in a groundloop crash.

4462

A measure of the lateral accelerations that may occur in a groundloop crash was provided by an experimental crash of a low-wing unpressurized transport airplane. This crash is shown by the sequence pictures of figures 9(a) and (b). The first crash impact simulated the unflared landings described previously. The impact speed of the airplane was 87 miles per hour, and the initial angle of impact with the ground was 12°. Following this initial impact, the airplane rebounded into the air and the left wing struck a series of poles. The resulting off-center drag turned the airplane until its longitudinal axis was about 20° to the mound of earth lying perpendicular to its path. The airplane struck this mound while still flying through the air and was lifted about 2 feet in passing over it. The plane then landed on its belly about 90 feet beyond the mound.

During this crash, the translational velocity of the airplane dropped from 87 miles per hour just before the airplane nose hit the ground initially to 74 miles per hour just after the airplane bounced into the air and the left wing tip first struck the series of poles. The velocity declined further to 63 miles per hour as the airplane turned through an angle of 70° when the wing contacted the poles. The second impact of the airplane occurred at this speed (fig. 9(c)). This indicates that 15 percent of the translational velocity of the airplane was removed by friction of the wing dragging along the earthen mound and by conversion to rotational velocity in turning the airplane.

Accelerations longitudinal, normal, and lateral to the airplane's axis were recorded during this crash. These data are shown following each picture sequence of the crash (figs. 9(a) and (b)). Data were recorded on the fuselage floor at stations 243 and 312 inches from the nose of the airplane. The accelerations experienced at station 312 at the moment of the second impact with the ground were 7 g's longitudinally, 28 g's normally, and 17 g's laterally. The accelerations for station 243 were 7 g's longitudinally, 40 g's normally, and 7 g's laterally. Since the airplane was at an angle when it hit the mound, these accelerations have been resolved to components parallel with the flight path of the

airplane as it approached the mound. This permits a comparison of the resulting acceleration with the longitudinal acceleration of the unflared-landing crashes. The accelerations parallel to the flight path during the groundloop crash were 19.0 g's at station 312 and 14.5 g's at station 243. The angle of impact of the airplane with the mound was estimated from a study of the motion pictures to be about 35°.

These data are corrected from an impact speed of 63 miles per hour to 95 miles per hour and compared with those of the unflared-landing crashes (fig. 5) in figure 10. The accelerations that resulted when the airplane struck the bank while moving sideways were essentially the same or only slightly higher than those that would have resulted from an unflared-landing crash at the same impact velocity. This result occurs despite the fact that the area of contact and the resistance to impact loads of the fuselage sides are quite different from those of the fuselage nose. That this horizontal acceleration compares with that of the unflared-landing crashes of comparable angle of impact may be purely fortuitous. Generalizations based on these comparisons are not warranted in view of the limited data.

An appreciation of the velocity that may be dissipated in rotating an airplane 180° can be obtained from the groundloop crash of a fighter airplane. A complete discussion of this crash is published in reference 3. Figure 11(a) shows sequence pictures of the action and the accelerations measured in the cockpit floor. During this crash, the velocity of the airplane dropped from 107 miles per hour when the nose first hit the ground to 60 miles per hour when the airplane hit the mound of earth while traveling backwards (fig. 11(b)). In this crash, 45 percent of the translational velocity was dissipated by friction or converted to rotational energy. When the airplane struck the mound of earth, the peak acceleration in the horizontal plane was only 11 g's (fig. 11(a)).

The fact that considerable velocity is lost in turning an airplane implies that significant forces must be applied to the airplane to turn it. If this force is not large, the airplane will not turn. The crash shown in figure 12(a) illustrates this point. During this crash, only the left landing gear was removed at the wheel barrier. This action tipped the airplane so that the left wing tip was dragging on the ground. Despite the force exerted by the dragging left wing tip, the airplane did not turn appreciably until its velocity had dropped from 89 to 43 miles per hour (fig. 12(b)). Even then the airplane only veered in its direction. The last half of the total rotation occurred after the airplane speed had decreased to about 8 miles per hour.

Another way in which crash loads can be applied from a direction other than the front is in a cartwheel crash. Such a crash is reported in reference 3. Sequence pictures and the recorded acceleration of the crash are shown in figure 13. The accelerations throughout this crash

4462

were low from all directions because of the wheel-like rotation of the airplane. The maximum acceleration recorded was 12 g's.

In order to obtain more information on the magnitude and direction of crash loads and the percentage of crashes in which loads from the various directions occurred in actual accidents, a study was made of about 100 CAB Accident Investigation Reports that were selected at random. The descriptions of the crashes were studied carefully, and the direction and magnitude of the crash forces were estimated. The magnitudes of the crash forces were classified in the following manner:

(1) No appreciable impact force

(2) Seats lightly loaded as in belly landing

(3) Some seat failures

(4) All seats collapsed or torn loose

(5) Some occupants killed by cabin crushing

The results of this study are shown in figure 14. Although this study is based upon an approximate estimate of the crash forces, the results show conclusively that the majority of severe crash impacts occur in crashes while the airplane is moving nose forward. There were no loads from the front of the airplane in only 2 percent of the crashes; whereas in 55 percent of the crashes there were no loads from the side, and in 94 percent of the crashes there were no loads from the rear of the airplane. Conversely, there were no crashes in which severe impact forces were applied from the rear of the airplane, and in only 6 percent of the crashes were there severe loads from the side (categories (4) and (5) of preceding force classification); but serious impact forces from the front were found in 39 percent of the crashes. Since the most severe crash impacts occur in a crash while the airplane is moving nose forward, the seats should be designed to have their maximum strength in this direction.

Although this study was based on a limited number of accident reports, and accidents have occurred that were not included in this study which had large crash forces from the rear, the results of the study do show conclusively that smaller crash loads would be expected from the side and rear of the airplane. This is consistent with the concept presented previously that considerable energy is lost in turning the airplanes. These crash accident data therefore support the view that, in most airplane crashes, the airplane first strikes in a direction parallel to its longitudinal axis and is apt to receive its greatest acceleration when loaded in this direction.

Effect of airplane configuration on horizontal accelerations. - The effect of crash attitude on the crash-impact hazard has been shown. The general arrangement of the major airplane components with respect to each other (the airplane configuration) also has an affect. The airplane configuration influences the degree of fuselage crushing that occurs during

a crash, and it can also affect the longitudinal accelerations that result. The configuration of the airplanes crashed in this investigation varied from that of the high-wing unpressurized transport, which had essentially an aluminum box suspended below the wing for a fuselage, to that of the low-wing pressurized airplane, which had a strong fuselage designed to resist pressurizing forces. Comparison of similar crashes with these varying airplane configurations will indicate the effect of wing location, fuselage design, and fuselage strength on the crash acceleration and fuselage crushing.

The effect of wing location in the vertical direction can be seen by comparing the data from crashes of the high-wing and the low-wing unpressurized transports at about 16° impact angle. The wing of the high-wing airplane with its elevated mass, including the powerplants and fuel, produces a large crushing force on the fuselage structure during the crash. The wing of the low-wing transport, however, strikes the ground first, so that the fuselage structure stops only its own mass. The crushing force on the fuselage of the low-wing airplane is therefore much smaller. Comparison of the crushing for these two crashes shows that the high-wing airplane fuselage is seriously crushed, the cargo-compartment floor and the weak nose section both collapsing extensively (fig. 15(a)). In a similar crash, the fuselage of the low-wing transport was hardly damaged (fig. 15(b)). The low-wing-transport impact speed was 109 miles per hour, whereas that of the high-wing airplane was only 91 miles per hour. The difference in fuselage damage is due primarily to the collapsing load applied by the wing of the high-wing airplane on the fuselage belly when it strikes the ground. It can be expected, therefore, other conditions being similar, that a high-wing airplane will be more likely to crush its occupants when involved in a crash.

The fore and aft location of the wing structure in low-wing airplanes also affects the possibility of crushing the occupants. If the wing structure and nacelles are located well forward on the fuselage and the angle of impact is not too steep, the wing structure will strike the ground first. The airplane will pitch up and slide without crushing the fuselage appreciably. If the fuselage extends well ahead of the wing structure, then the forepart of the fuselage must stop the whole airplane, as was the case for the high-wing airplane. If the fuselage structure is weak, the fuselage may crush back to the wing.

The 16° unflared-landing crash of the unpressurized low-wing transport (fig. 15(b)) and the 15° crash of the low-wing pressurized transport (fig. 3(b)) illustrate the kinematics just discussed. As shown previously in the crash of the unpressurized airplane, the wings hit the ground first and the fuselage did not crush (fig. 15(c)). In the crash of the pressurized transport also shown previously, the fuselage nose struck the ground first; however, because of its high strength, the fuselage was not crushed excessively. If the fuselage strength had been comparable to that of the unpressurized airplane, the fuselage would probably have been crushed extensively.

4462 CK-2

The longitudinal crash accelerations may also be affected by the configuration of the airplane. Any airplane design features that tend to produce sharp edges or projections supported by strong structure that can plow into the ground may increase the longitudinal accelerations during a crash. Conversely, any design feature that helps to maintain smooth planing surfaces will tend to reduce the acceleration. The fuselage of the high-wing airplane provides an example of a design that tends to increase the accelerations. The nose section of the airplane is essentially a fairing that carries only aerodynamic loads (fig. 2(c)). However, the fuselage floor structure proper is much stronger because of the integrated fore and aft keel and cargo floor structure. During the 16° unflared-landing crash, the nose section crumpled back until the sharp front edge of the floor structure dug into the ground. During this crumpling of soft structure, the longitudinal acceleration gradually increased. When the floor structure hit the ground, a peak of about 15 g's was sustained intermittently for about 0.05 second (fig. 15(a)). Relatively high accelerations were also obtained during the 4° high-wing-airplane crash (fig. 16). In this crash, an acceleration of 6 g's was obtained, compared with 2.5 g's for the 5° crash of the low-wing pressurized transport (fig. 3(a)).

4462

The 16°-impact-angle crash of the low-wing unpressurized transport provides an example in which the fuselage did not crush. However, sharp plowing edges were formed by the relatively strong engine nacelles that plowed the ground. The acceleration in this crash reached peak values of 15 and 13 g's for station 243 and 312, respectively (fig. 15(b)). These values are approximately the same as those obtained in the 16° high-wing-airplane crash (fig. 15(a)). However, the high-wing-transport impact speed was 18 miles per hour slower than that of the low-wing transport.

The pressurized airplane with its strong fuselage structure in relation to the airplane weight, on the other hand, retained a comparatively smooth planing undersurface when subjected to a 15° crash (fig. 8(b)). When the nose of the airplane hit the ground, it did not crush appreciably. Instead, the airplane pitched up and slid on its belly up the hill. Since there were few sharp edges plowing the ground, the maximum accelerations obtained at four locations on the floor averaged only 9 g's (fig. 4(a)), compared with 15 g's for the low-wing unpressurized airplane. Even when the pressurized transport was crashed at an angle of impact of 29°, the destruction of the fuselage nose was minor, so that there was a relatively smooth planing surface (fig. 8(c)). The accelerations in this crash were low considering the angle of impact of the crash; the peak acceleration averaged only 20 g's (fig. 4(b)).

Another crash in which there was very little plowing of the ground was the low-wing unpressurized-transport crash at 12° angle of impact (fig. 9(a)). In this crash, the wing structure hit the ground first and the nacelles did not plow the ground. The acceleration measured on the

fuselage floor was only 3.5 g's. The impact speed of the crash was 87 miles per hour.

In figure 17 the acceleration data discussed are corrected to a common impact speed of 95 miles per hour and superimposed on the data of figure 5. The low-wing unpressurized transport in the 12°-crash impact had the least plowing and the smallest acceleration at this impact angle. The three pressurized airplanes also show relatively small accelerations because the plowing action also was minor. Somewhat more plowing occurred in the 16° low-wing unpressurized-airplane crash, because the nacelles plowed the ground. The resulting acceleration was greater than that for the pressurized-airplane crashes. The greatest accelerations occurred during the high-wing unpressurized-transport crashes when the soft nose structure of the airplane crushed against the floor structure and the sharp edges plowed into the ground, as in the 4° and 16° crashes.

The data obtained during the crashes of the fighter airplanes in reference 3 are also included in figure 17. Four unflared-landing crashes were made at angles of impact 4°, 18°, 22°, and 27°. The impact speed in all cases was approximately 110 miles per hour. The data for the fighter crashes fall well above the data for both low-wing transports. However, the data for the fighter crashes show almost the same relation as obtained with the high-wing unpressurized transport. Extremely severe plowing of the fuselage occurred in these fighter crashes. The airplane had a nose fairing in front of the cockpit section. This nose fairing broke off in the three higher impact crashes and was deformed in the groundloop crash, in which the initial angle of impact was 4°. This exposed a very sharp plowing edge that was supported by the strong cockpit structure. Sequence pictures of these crashes are shown in figures 11(a) and 18.

The agreement between the data for the fighter and high-wing transport airplanes is interesting, because it suggests that the size of the airplane does not have a major effect in determining the accelerations that result from a crash. Both of these airplanes develop sharp plowing edges during crash that are supported by strong structure. In order to say conclusively that the size of the airplane has no effect, it would be necessary to establish that the degree of plowing was the same for the fighter and the high-wing airplanes. This is not possible, for no measure of this variable was obtained in this investigation. Inspection of the airplane damage for the fighter and high-wing airplanes showed, however, that they both presented major structural members that served as plows. It appears that these plowing members have a size and strength that are proportional to the weight of the airplane. The resulting accelerations of the two airplanes therefore tended to be the same despite the difference in size.

In regard to this conclusion it is necessary to distinguish between the acceleration resulting from impact with ground-supported obstructions such as trees and boulders and the acceleration resulting from impact with

4462

CK-2 back

the ground itself. While plowing of the ground provides accelerations that are related to the strength of the plowing element, the acceleration that occurs when the airplane strikes ground-supported objects is related to the strength of these objects or the strength of the local airplane structure that contacts the obstructions. For a given ground-supported object that breaks, the airplane acceleration will decline as the mass of the airplane increases, since the breaking force is constant. If the ground-supported obstacle does not break, then the acceleration will depend on the strength of the local airplane structure in contact with the obstacle and the weight of the airplane. No general rule governing the relation between airplane weight and acceleration can be stated under these circumstances.

4462

In relation to the effect of size of the airplane, some further data of interest were obtained with 1200-pound cub-type light airplanes (ref. 1). These airplanes were crashed into a 55° slope at speeds of 60, 47, and 42 miles per hour. Sequence pictures of one of these crashes are shown in figure 19. If the resulting accelerations are corrected to 95 miles per hour, accelerations of 48 and 50 g's are obtained at a 55° angle of impact. These data points are also plotted in figure 17. These accelerations show the same general trend that was obtained with much bigger airplanes.

Shape and duration of longitudinal acceleration pulses. - The acceleration pulses recorded during this investigation as a result of the first impact of the airplane with the ground may be represented approximately by a half sine wave. The duration of these pulses appears to have a random nature, which makes analysis difficult. The durations of the pulses are listed in table I. These durations vary from about 0.1 to 0.3 second. As long as the acceleration in a crash is less than the human tolerance limit for severe injury, as indicated in reference 6, this variation in duration is of little consequence. If the acceleration exceeds the human tolerance limits, undoubtedly this variation in duration would have an effect on the injury received.

Concluding remarks on horizontal acceleration. - From the data presented on the effect of airplane configuration, it may be concluded that the location of the wing is important in reducing both the degree of fuselage crushing and the acceleration that result from a crash. High-wing airplanes that have weak fuselage structures may be crushed extensively during a crash. If the cabin structure is made stronger but a soft nose structure is retained, the crushing may be reduced but the acceleration may be fairly large because of the large plowing edge that may be formed on destruction of the nose. In contrast, if the structure that initially hits the ground is strong and does not crush extensively during the crash, so that a relatively smooth planing surface remains, relatively low longitudinal acceleration will result.

One of the many considerations required for the selection of a design acceleration for seats and their attachments is a knowledge of the maximum acceleration the airplane can withstand. Unfortunately, the crashes of this study were not severe enough to indicate the maximum strength of the pressurized transport airplane. However, during the 29° pressurized-transport crash a maximum of 20 g's was recorded on the fuselage floor, yet only minor damage to the fuselage resulted. The airplane can obviously withstand a more severe crash without crushing the occupied compartments. During the crash of the same type of airplane at Louisville, Kentucky, which crashed at an estimated impact angle of 50° and a speed of 150 miles per hour, living space remained in the aft part of the airplane.

In concluding this discussion of acceleration in the horizontal plane of the airplane it must be pointed out that the data presented herein are for the acceleration of the floor of the airplane. The acceleration of the seat and its occupant may be of the same magnitude, or of greater or less magnitude, depending on the dynamic response of the seat and restraining harness. This is also true for the normal accelerations that are presented in the next section.

Normal Accelerations

The magnitude of the normal accelerations (perpendicular to lateral and longitudinal airplane axes) from point to point in the fuselage of an airplane during a crash varies considerably depending on the motion of the airplane. If the airplane strikes a surface in a manner similar to an unflared landing, the impact will pitch the fuselage up and force the airplane to rotate about a lateral axis. This pitching motion will affect the normal accelerations from position to position in the fuselage. Such pitching motion was present in these experimental crashes. It is possible therefore to obtain an indication of its effect on the variation of the normal acceleration with position in the airplane.

The motion described can be seen in figures 3(b) and (c). The succession of photographs shows that in each crash the nose of the airplane is deflected upward and the fuselage appears to rotate about a lateral axis. This action continues until the path of the airplane is parallel to the slope of the ground. Study of this action in slow-motion pictures shows that the trajectory of the fuselage nose changes more rapidly than that of other parts of the airplane. This effect can be seen in figure 20, which shows a plot of the trajectory of a point on the aft part of the fuselage and the angle of the fuselage longitudinal axis to the horizon. Because of this rotation, the normal acceleration should be the greatest at the impact point and should decrease as the distance from the impact point increases.

The normal accelerations measured in the fuselage floor during the 15° and 29° crashes of the pressurized transport are shown in figures 3(b) and (c). The variation of the maximum normal acceleration with distance from the impact point on the airplane is shown in figure 21. In the 29° crash at a point 460 inches from the impact point, the normal acceleration was only about half that which occurred at a point 155 inches from the impact point. In the forward part of the airplane the acceleration decreases linearly with distance from the impact point as a result of the rotation of the airplane. The acceleration farther aft, 655 inches from the impact point, does not decrease linearly. The acceleration at this aft station is larger because the tail of the airplane hit the level ground at the foot of the slope and stopped the rotation of the airplane (fig. 20).

The same decrease in normal acceleration with distance from the impact point was noted in the 15° crash of the pressurized transport. The data for this crash are also shown in figure 21. However, the general slope of the line is less than for the 29° crash.

Effect of crash angle of impact on normal acceleration. - An indication of the effect of impact angle on the normal acceleration can be obtained by cross-plotting the data of figure 21 at various distances from the impact point, as in figure 22. The normal acceleration increases as the angle between the airplane's path and the surface it strikes becomes greater. The appendix to this report shows that this relation would be expected to continue up to an impact angle of about 35°, as a result of the relation between the plowing and friction forces. Beyond this angle the normal acceleration decreases. At an angle of about 73° the normal component again becomes zero. At this point the resultant of the forces normal and parallel to the inclined surface is in line with the trajectory of the airplane. Therefore, there is no component of the force tending to raise the airplane.

The data of figure 22 also show that the normal acceleration increases more rapidly in the forward part of the airplane as the impact angle becomes steeper. The curves indicate that at an impact angle of 30° the normal acceleration is 23 g's 200 inches from the impact point, but only 11 g's 600 inches from the impact point.

The largest normal acceleration that would be expected in crashes of the pressurized airplane used in this investigation can be obtained by cross-plotting the data of figure 22 at 35° angle of impact, as in figure 23. The curve indicates that the floor in a forward part of the airplane, less than 300 inches from the point of impact, will be exposed to normal accelerations greater than 20 g's. Such accelerations exceed human tolerances without injury (ref. 6). The floor aft of 300 inches from the point of impact would not be subjected to acceleration exceeding 20 g's in crashes.

Effect of airplane configuration on normal acceleration. - The airplane configuration may affect the normal as well as the longitudinal accelerations. In figure 24 the maximum normal accelerations obtained in the crashes of the high- and low-wing unpressurized airplanes (figs. 9(a), 9(b), 15(a), 15(b), and 16) are combined with the data for the pressurized airplane (fig. 21). These data, which are corrected to an impact speed of 95 miles per hour in the same manner as were the longitudinal accelerations, indicate that the important variables affecting the normal acceleration are angle of impact and distance from the impact point. The airplane configuration appears to have a relatively minor effect upon the normal acceleration in the crashes studied. Except for the one data point for the 4° crash of the high-wing transport, the data are consistent with the family of curves shown in figure 22. The data for the 4° crash of the high-wing airplane are slightly higher than those indicated for the 4° curve. The data for the 16° crash of the high-wing airplane are slightly higher than those obtained in the 15° crash of the pressurized airplane, as would be expected. The data for the 12° and 16° low-wing unpressurized-airplane crashes also fall reasonably well in line with the data for the pressurized airplane.

4462

From the data presented in the previous sections it is apparent that modern transport airplanes are capable of withstanding normal accelerations without extensive fuselage crushing that are higher than the human body can tolerate without serious injury or fatalities. This is particularly true near the point of impact on the airplane.

Shape and duration of normal acceleration pulses. - The shape of the normal acceleration pulses on the floor is quite irregular, and these pulses cannot be represented simply as the longitudinal pulses were. The acceleration as a result of the first impact of the airplane with the ground has several peaks. The duration of the pulses is also difficult to determine because of the irregularity of the pulses. Approximate values for the duration of the pulses are listed in table I. The duration of the normal pulse varies over a relatively narrow range. Values from about 0.07 to 0.35 second were obtained. This small range would be of little consequence as long as the accelerations are less than the human tolerance limits for severe injury.

CONCLUSIONS

From the data of this investigation, the following conclusions can be drawn:

1. Pressurized transport airplanes can withstand high-impact-angle crashes and still maintain survivable areas within the fuselage. During the 29° unflared-landing crash of this investigation, a maximum of 20 g's longitudinal acceleration was recorded on the fuselage floor, and only minor damage to the fuselage resulted.

2. During unflared-landing crashes greater fuselage crushing will occur with high-wing than with low-wing airplanes.

3. Airplanes with strong fuselage structures that do not deform and produce sharp, well-supported plowing edges will have relatively low longitudinal acceleration during crashes similar to those studied.

4. Normal accelerations are greatest near the point of impact of the airplane with the ground.

5. Normal accelerations exceeding human tolerance without injury can occur in crashes in which modest fuselage damage occurs.

6. The configuration of the airplane had little effect on the normal accelerations measured in this study.

Lewis Flight Propulsion Laboratory
National Advisory Committee for Aeronautics
Cleveland, Ohio, November 13, 1957

APPENDIX - VARIATION OF CRASH-IMPACT FORCES NORMAL TO LONGITUDINAL AXIS WITH ANGLE OF IMPACT

The crash data presented in this report indicate that the magnitude of the crash-impact forces normal to the plane of the longitudinal and lateral axes varies with impact angle and with location in the airplane. However, the range of impact angles in the crash data is not adequate to indicate the impact angle at which the maximum normal acceleration occurs and the general relation between impact angle and normal acceleration. It is therefore desirable to obtain an indication of this relation analytically.

The simplified crash situation shown by figure 25 is analyzed. The path of the airplane is assumed to be horizontal. The longitudinal axis of the airplane is also assumed to be horizontal. A surface inclined at an angle i with the horizontal lies in the path of the airplane. The angle i is thus also the angle of impact of the airplane with the ground. It is further assumed that the mass of the airplane is concentrated near the point on the airplane that first touches the ground. This assumption is only a gross approximation, because during the crashes studied sufficient moment was applied to the airplane at impact to rotate it about a lateral axis. However, since this analysis is to be used only to make a short extrapolation of the data obtained, this assumption is believed to be justified for simplicity.

When the airplane strikes the inclined surface, aerodynamic, crumpling, resilient, friction, soil compression, and plowing forces will change the path of the airplane until it is sliding parallel to the inclined surface. The aerodynamic forces are assumed negligible and are disregarded in this discussion. It is further assumed that airplane crashes of the type being discussed are essentially nonelastic and therefore the resilient forces can generally be neglected. The force of soil compression and the force of crumpling the fuselage structure are equal and opposite. Consequently, only the crumpling, plowing, and friction forces are considered in this discussion.

The relation of the crumpling, plowing, and friction forces with respect to the longitudinal axis of the airplane is shown in figure 25. Because of contact between the inclined surface and the fuselage structure, the fuselage will collapse and decrease the velocity normal to the inclined surface. It is assumed for this discussion that this force can be expressed by the relation

$$F_{ns} = \alpha s_c A_c \tag{1}$$

4462 CK-3

where F_{ns} is the force perpendicular to the inclined surface that crumples the fuselage structure, s_c is the distance the fuselage collapses perpendicular to the inclined surface, α is the coefficient of compression of the fuselage structure, and A_c is the fuselage area in contact with the inclined surface.

In addition to the force normal to the inclined surface, there also will be plowing and friction forces parallel to the inclined surface. As the airplane slides forward, the soil ahead of the airplane will be plowed by projecting parts of the airplane structure. Plowing of the soil thus introduces a force parallel to the inclined surface. This plowing force depends upon the cross-sectional area of the furrows. It is assumed that the plowing force parallel to the inclined surface can be expressed as

$$F_{ps(plowing)} = \mu A_p$$

where A_p is the cross-sectional area of the plowed furrows and μ is the plowing force per unit area.

The frictional force resulting from the sliding of the fuselage skin on the material of the inclined surface is given by the relation

$$F_{ps(friction)} = \eta F_{ns}$$

where η is the friction coefficient for aluminum sliding on the material of which the inclined surface is composed.

The total force parallel to the inclined surface is then the sum of the forces just described or

$$F_{ps} = F_{ps(plowing)} + F_{ps(friction)} = \mu A_p + \eta F_{ns}$$

Substituting equation (1) for F_{ns} gives

$$F_{ps} = \mu A_p + \eta \alpha s_c A_c \qquad (2)$$

The forces perpendicular and parallel to the inclined surface each have components normal to a plane including the longitudinal and lateral axes of the airplane. It is the effect of impact angle upon this maximum normal force that is to be determined. From figure 25, it can be seen that this normal force is composed of components of the forces normal and parallel to the inclined surface. This force can be stated as

$$F_{na} = F_{ns} \cos i - F_{ps} \sin i \qquad (3)$$

4462

Substituting the values for the forces normal and parallel to the inclined surface from equations (1) and (2) in equation (3) gives

$$F_{na} = \alpha s_c A_c \cos i - (\mu A_p + \eta \alpha s_c A_c) \sin i \qquad (4)$$

The distance the fuselage collapses s_c in equation (4) depends upon the kinetic energy of the airplane normal to the inclined surface. The kinetic energy normal to the inclined surface is dissipated in collapsing the fuselage structure and compressing the soil under the fuselage. The kinetic-energy loss can therefore be equated to the work done in collapsing the fuselage structure and compressing the soil,

$$\frac{1}{2} M V_n^2 = \int F_{ns} \, ds_c + \int F_{comp} \, ds_s$$

where

M mass of airplane

V_n initial velocity normal to inclined surface

F_{comp} force of compression of soil

s_s distance soil is compressed normal to inclined surface

Since $F_{ns} = F_{comp}$,

$$\frac{1}{2} M V_n^2 = \int F_{ns} \, ds_T$$

where $s_T = s_c + s_s$. Since $F_{ns} = \alpha s_c A_c$,

$$\frac{1}{2} M V_n^2 = \int \alpha s_c A_c \, ds_T$$

Since $F_{comp} = \beta s_s A_c$, where β is the coefficient of soil compression, and $F_{ns} = F_{comp}$, then

$$\alpha s_c = \beta s_s$$

$$s_c = s_T - s_s = s_T - \frac{\alpha s_c}{\beta}$$

$$s_c = \frac{s_T}{1 + \frac{\alpha}{\beta}}$$

4462 CK-3 back

Then

$$\frac{1}{2} MV_n^2 = \int \frac{\alpha s_T A_c}{1 + \frac{\alpha}{\beta}} ds_T$$

Integrating and assuming appropriate average values for A_c, α, and β that are therefore constant yield

$$MV_n^2 = \frac{\alpha A_c}{1 + \frac{\alpha}{\beta}} s_T^2$$

4462

Since $s_T = s_c \left(1 + \frac{\alpha}{\beta}\right)$, and $V_n = V \sin i$,

$$s_c = V\left[\frac{M}{\alpha A_c\left(1 + \frac{\alpha}{\beta}\right)}\right]^{1/2} \sin i$$

Substituting this value for s_c in equation (4), clearing, and collecting terms give

$$F_{na} = \left(\frac{\alpha A_c M}{1 + \frac{\alpha}{\beta}}\right)^{1/2} V \sin i \cos i - \mu A_p \sin i - \left(\frac{\alpha A_c M}{1 + \frac{\alpha}{\beta}}\right)^{1/2} \eta V \sin^2 i \qquad (5)$$

This equation gives the maximum force that will be produced in unflared-landing crashes in a direction normal to the longitudinal axis of the airplane on the fuselage floor above the point of impact.

The data obtained in this investigation can be extrapolated by applying equation (5). The equation can be used by simplifying it to the form

$$F_{na} = K_1 \sin i \cos i - K_2 \sin i - \eta K_1 \sin^2 i$$

The constants K_1 and K_2 can then be evaluated by using the crash data. Equation (5) indicates the magnitude of the normal force in the airplane directly above the point of impact. The crash data apply to points on the fuselage floor at varying distances from the impact point. For this reason, the data of figure 22 have been cross-plotted at impact angles of 10°, 20°, and 30° and the curves extended to the point of impact in figure 26. At the point of impact, normal accelerations of 18.5, 32, and 40 g's were obtained for impact angles of 10°, 20°, and 30°, respectively. From the laws of motion, it is known that $F_{na} = Wg$, where W

is the weight of the airplane and g is the acceleration in gravity units. Also, experiments have shown that, for aluminum sliding on clay (the crash site was predominantly clay), η is approximately 0.3. Substituting these values in equation (5) to obtain simultaneous equations and solving gave values of $K_1 = 113.2$ and $K_2 = 0.913$.

The resulting equation is

$$g = 113.2 \sin i \cos i - 0.913 \sin i - 33.96 \sin^2 i \qquad (6)$$

4462

This equation is plotted in figure 27. This curve indicates that the normal acceleration increases with impact angle and that for the crashes studied the maximum normal acceleration will occur at 35° angle of impact. The curve also indicates that beyond this angle of maximum normal acceleration the normal acceleration decreases with further increase in impact angle and becomes zero again at about 73°.

Equation (6) thus gives the general relation between maximum acceleration and impact angle when used in conjunction with the crash data. This equation should not, however, be used to calculate the magnitude of the accelerations in crashes involving different circumstances and different airplanes.

With the curve obtained from equation (6) the data from figure 22 can be extrapolated from 29° to the angle of impact for maximum acceleration. This extrapolation is based upon the assumption that the proportionality between the normal acceleration at various stations in the fuselage and that obtained at the point of impact shown by figure 27 will continue through the angle of impact for maximum acceleration. This extrapolation is shown by the dashed lines in figure 27.

As an interesting extension of the analysis, values for the terms of equation (5) were estimated for the 29°-angle-of-impact crash of the pressurized transport by an inspection of the crashed airplane and crash site. The following values were obtained:

$$M = 1172 \text{ slugs}$$

$$A_p = 3 \text{ sq ft}$$

$$A_c = 110 \text{ sq ft}$$

$$V = 146 \text{ ft/sec}$$

$\beta = 300{,}000$ (lb/sq ft) ft (from pentrometer readings at crash site)

With these values and equation (5), the following values were obtained for the coefficients:

$$\alpha = 6800 \text{ (lb/sq ft) ft}$$

$$\mu = 11{,}500 \text{ lb/sq ft}$$

This method of calculation indicates that the fuselage belly structure under the nose and wing will collapse 1 foot when loaded with 6800 pounds per square foot. This is the strength of the fuselage underbelly while this structure is also being destroyed by the plowing and friction forces parallel to the ground.

The value of μ (11,500 lb/sq ft) is of the same order of magnitude as that obtained in preliminary tests conducted by the NACA Lewis laboratory. In these tests, a V-shaped plow was dragged along the ground and the plowing force recorded. Values for μ in these experiments varied from 7200 to 9000. It thus appears that the value of 11,500 obtained in the analysis is reasonable.

4462

REFERENCES

1. Eiband, A. Martin, Simpkinson, Scott H., and Black, Dugald O.: Accelerations and Passenger Harness Loads Measured in Full-Scale Light-Airplane Crashes. NACA TN 2991, 1953.

2. Preston, G. Merritt, and Eiband, A. Martin: Crash Impact Survival in Light Airplanes. NACA Tech. Film No. 25, 1955.

3. Acker, Loren W., Black, Dugald O., and Moser, Jacob C.: Acceleration in Fighter-Airplane Crashes. NACA RM E57G11, 1957.

4. Black, Dugald O.: Facilities and Methods Used in Full-Scale Airplane Crash-Fire Investigation. NACA RM E51L06, 1952.

5. Civil Aeronautics Board: Accident Investigation Report. File No. 1-0079, Aug. 18, 1954.

6. Pesman, Gerard J., and Eiband, A. Martin: Crash Injury. NACA TN 3775, 1956.

TABLE I. - ACCELERATION OF FLOOR

Transport	Impact angle, deg	Impact velocity, mph	Impact point, distance from airplane nose, in.	Location of accelerometers, distance from airplane nose, in.	Accelerations						Acceleration corrected to 95-mph impact velocity		Average duration of pulse	
					Longitudinal		Normal		Lateral					
					Magnitude of peak, g	Time of peak, sec	Magnitude of peak, g	Time of peak, sec	Magnitude of peak, g	Time of peak, sec	Average longitudinal, g	Normal, g	Longitudinal, sec	Normal, sec
Low-wing pressurized	5	81	805	270	2.5	0.190	2.8	0.265			2.9	2.9	0.35	0.38
	15	93	80	250	10	0.120	15	0.095			9.3	15.3	0.22	0.18
				380	11	.122	10	.075				10.2		
				488	7	.125	10	.150				10.2		
				680	9	.125	8	.170				8.2		
	29	97	30	185	20	0.145	25	0.105-0.175			19.3	24.4	0.23	0.21
				335	22	.145	18	.135				17.6		
				490	20	.150	12.5	.160				12.2		
				685	17	.155	10	.195				9.8		
Low-wing unpressurized	12	97	108	243	3.5	0.285	9	0.275			5.8	9.9	0.12	0.09
				312	3.5	.260	9	.275				9.9		
		65	172	243	7	1.653	40	1.653	7	1.653	10.5	6.0	0.13	0.13
				312	7	1.680	28	1.680	17	1.680		4.2		
	18	109	72	243	15	0.195	18	0.180			12.2	15.7	0.25	0.22
				312	13	.185	18	.215				14.0		
High-wing unpressurized	4	95	158	Long 138, norm 140	8	0.150	12	0.050			8	12	0.17	0.17
	18	91	56	Long 340, norm 341	15	0.070	10	0.300			15.7	10.5	0.10	0.07

4462

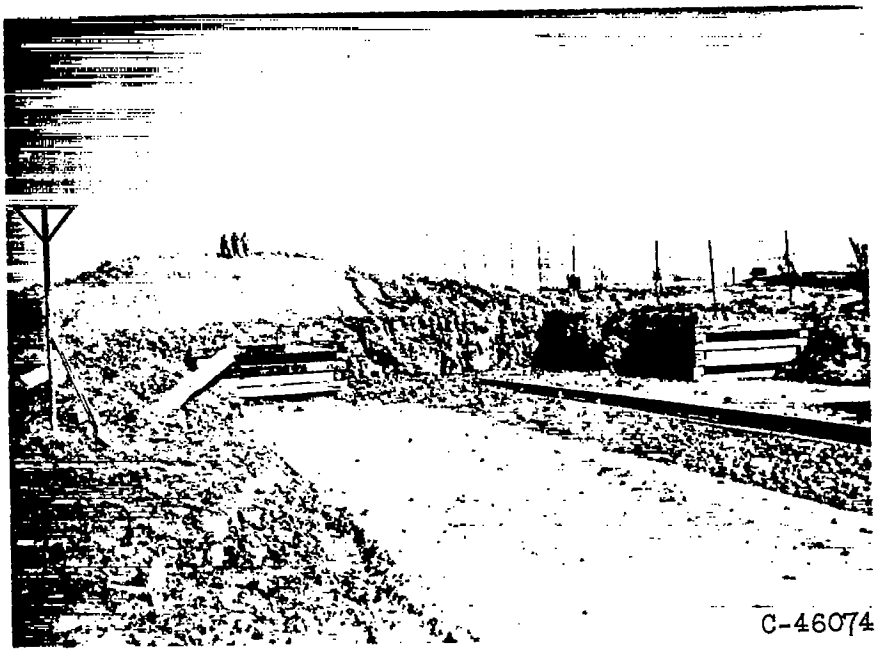

(a) Earth and timber abutments that ripped landing gear from airplane upon crash.

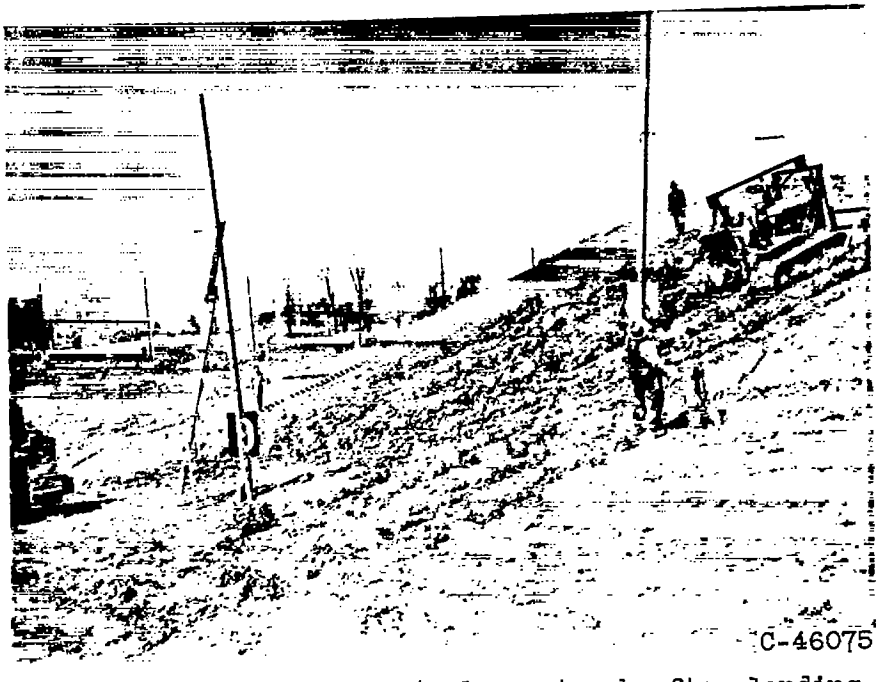

(b) Earthen mound that airplane struck after landing gear was removed.

Figure 1. - Site of crash investigation.

4462

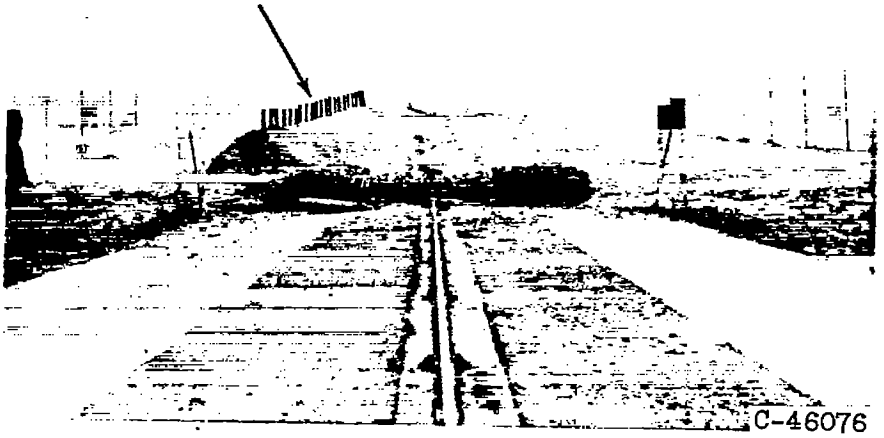

(c) Wing barrier used to produce groundloop crash.

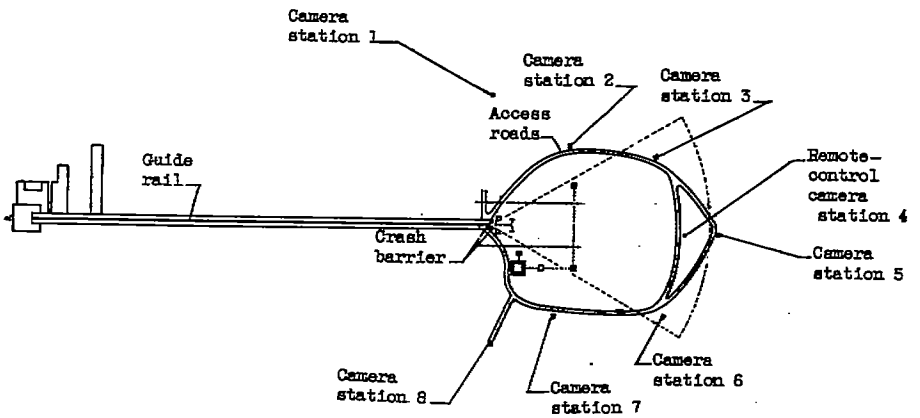

(d) Plan view of test site.

Figure 1. - Concluded. Site of crash investigation.

CK-4

4462

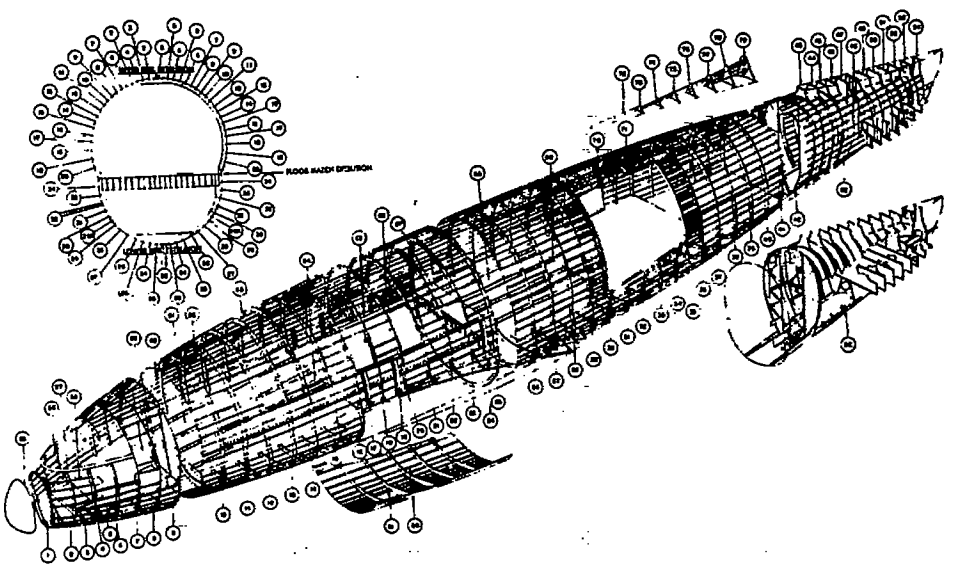

(a) Pressurized low-wing transport.

Figure 2. - Photographs and diagrams of fuselage structures of transport airplanes crashed in impact-survival investigation.

4462
CK-4, back

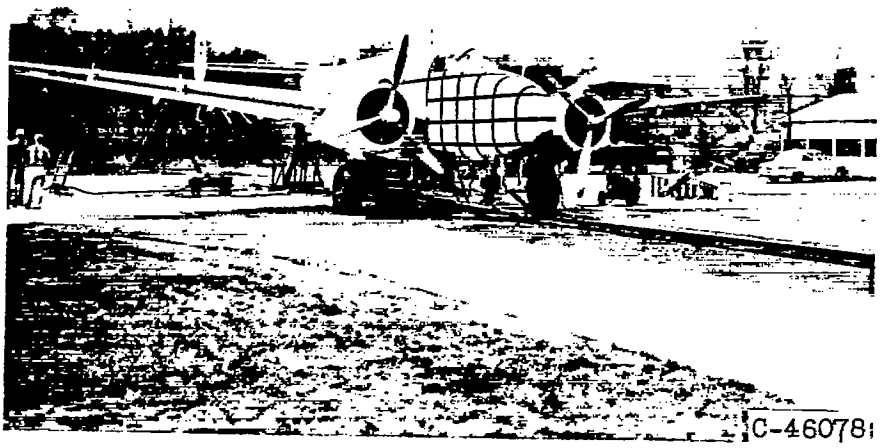

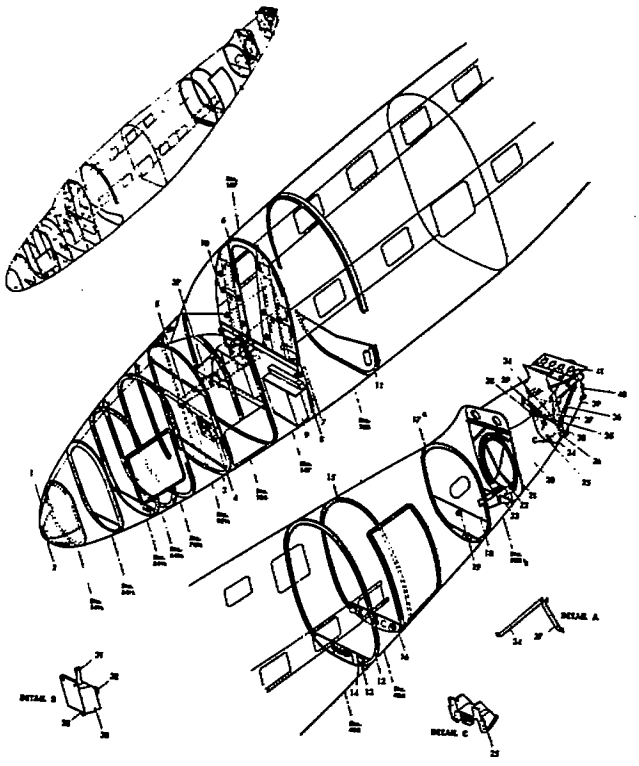

(b) Unpressurized low-wing transport.

Figure 2. - Continued. Photographs and diagrams of fuselage structures of transport airplanes crashed in impact-survival investigation.

4462

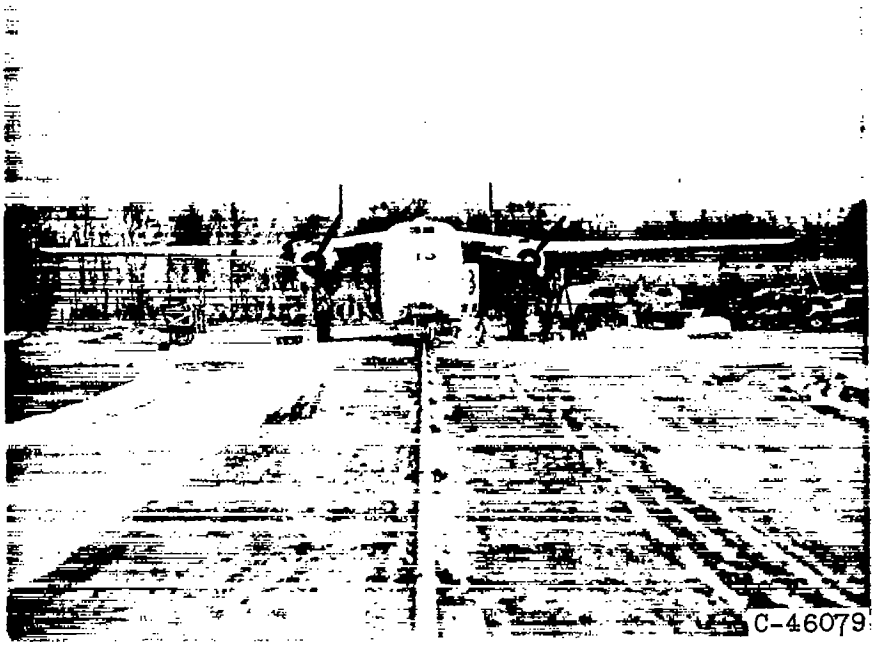

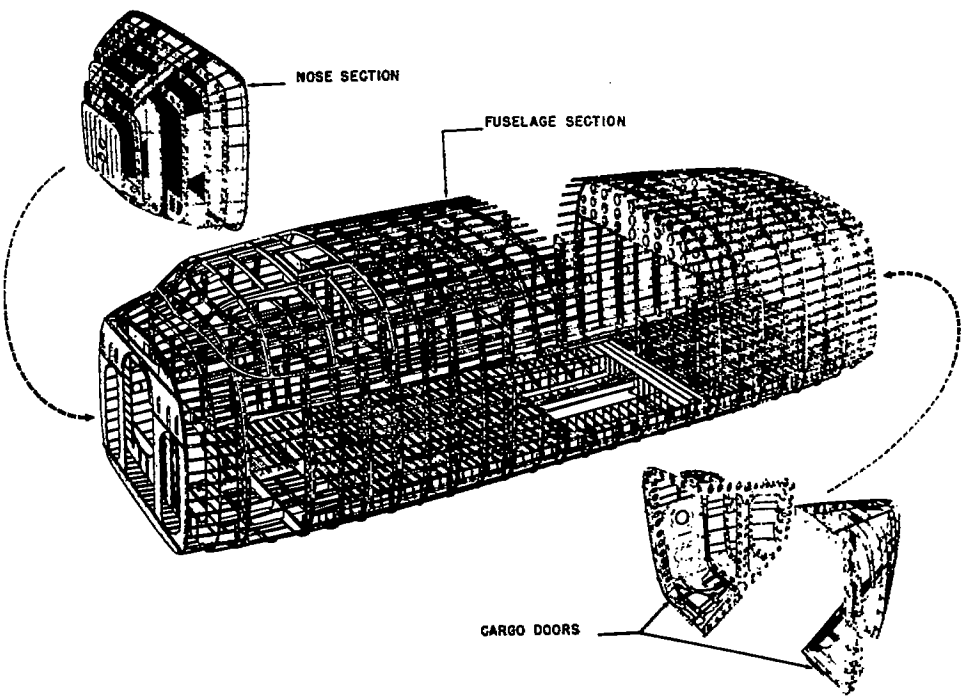

(c) Unpressurized high-wing transport.

Figure 2. - Concluded. Photographs and diagrams of fuselage structures of transport airplanes crashed in impact-survival investigation.

0 Sec 0.08 Sec 0.17 Sec

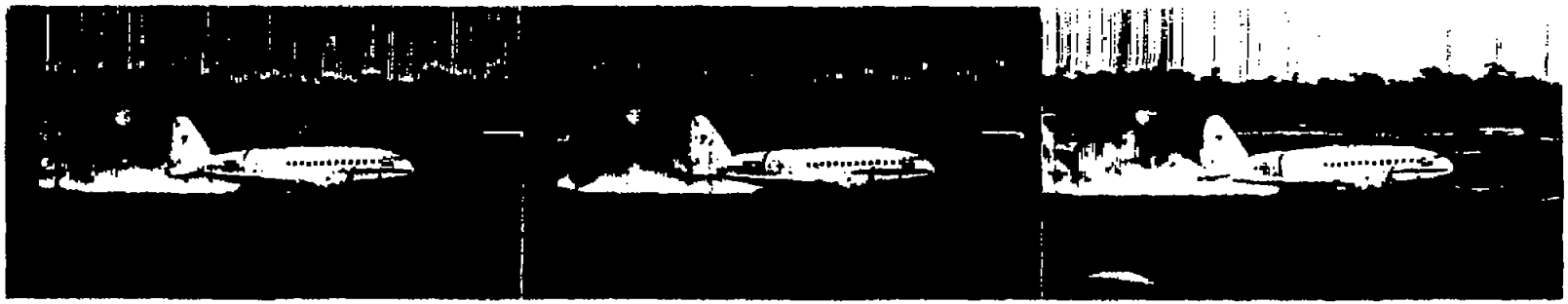

0.25 Sec 0.33 Sec 0.42 Sec

C-46080

0.50 Sec 0.58 Sec

(a) Angle of impact, 5°; impact speed, 81 mph.

Figure 3. - Sequence pictures and accelerations of crashes of pressurized transports. (Zero time is fuselage nose impact with ground.)

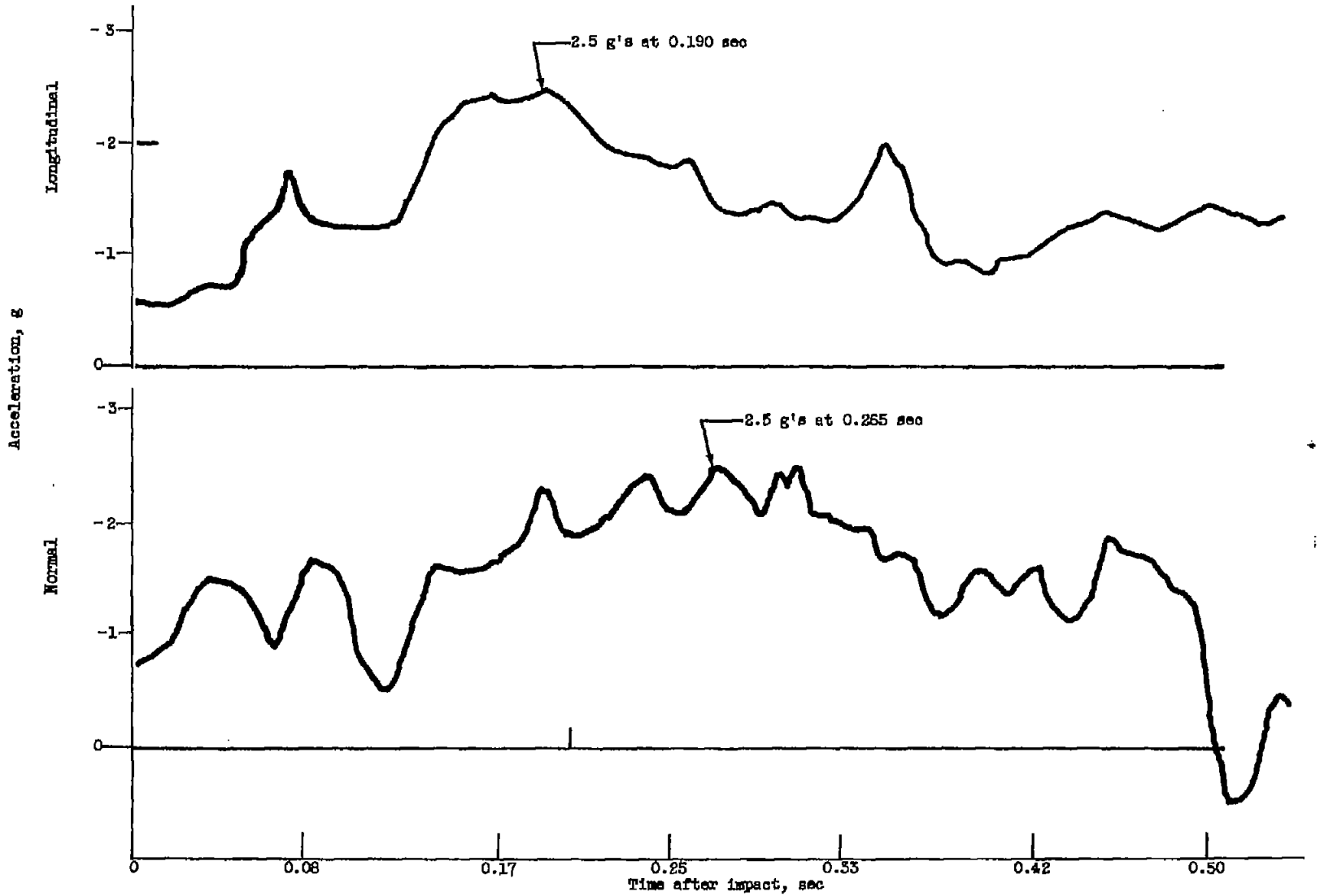

(a) Concluded. Angle of impact, 5°; impact speed, 81 mph.

Figure 3. - Continued. Sequence pictures and accelerations of crashes of pressurized transports. (Zero time is fuselage nose impact with ground.)

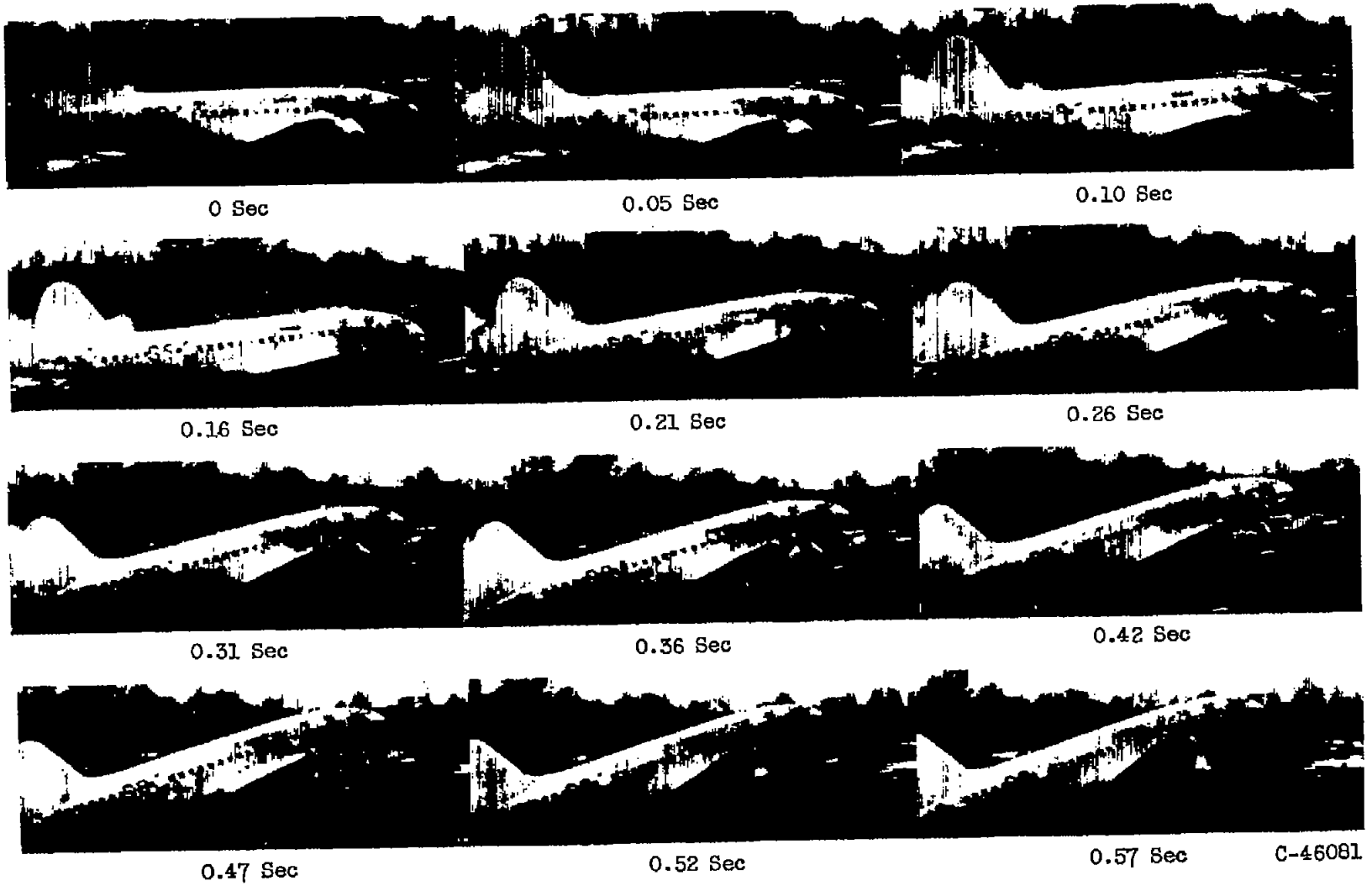

(b) Angle of impact, 15°; impact speed, 93 mph.

Figure 3. - Continued. Sequence pictures and accelerations of crashes of pressurized transports. (Zero time is fuselage nose impact with ground.)

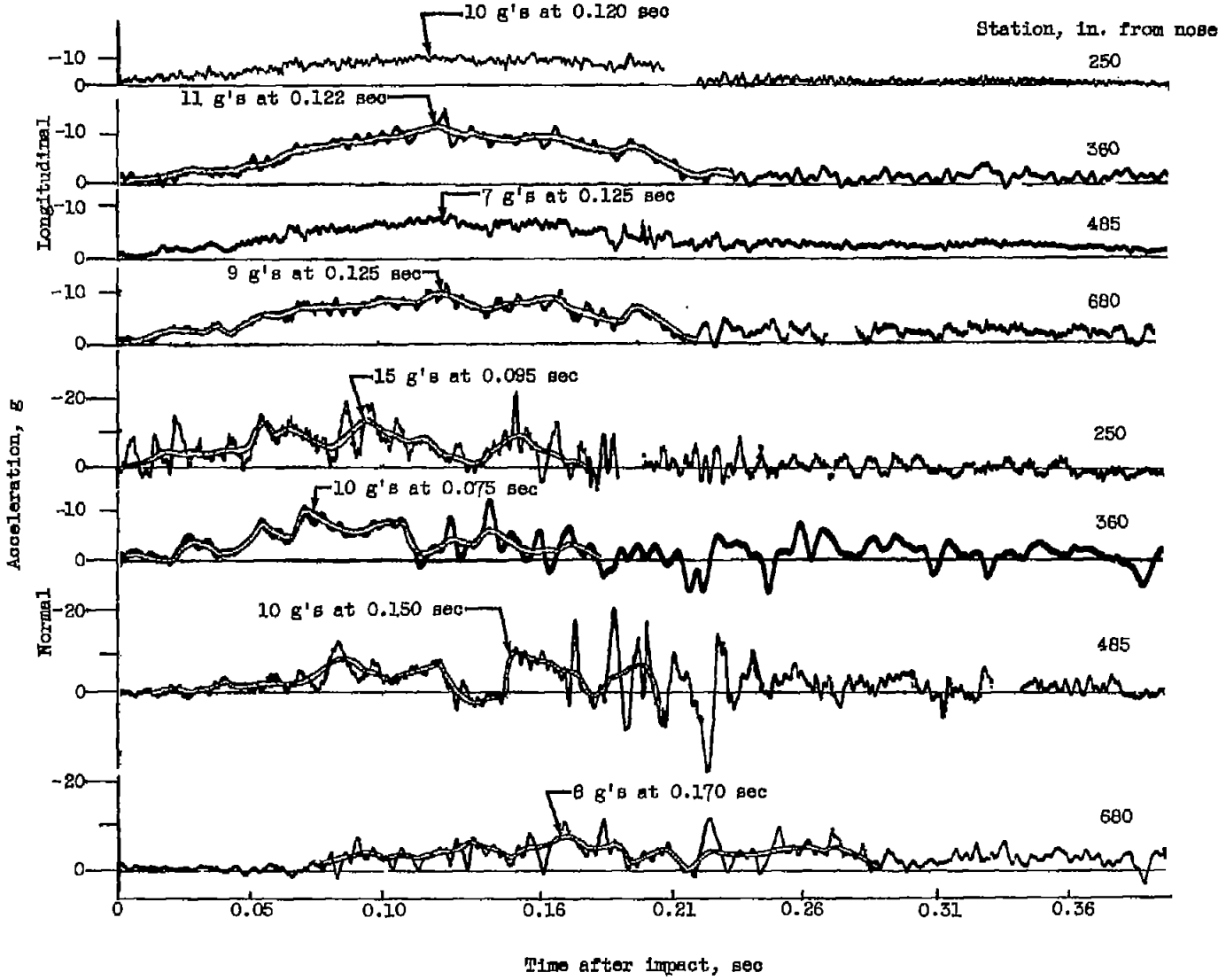

(b) Concluded. Angle of impact, 15°; impact speed, 93 mph.

Figure 3. - Continued. Sequence pictures and accelerations of crashes of pressurized transports. (Zero time is fuselage nose impact with ground.)

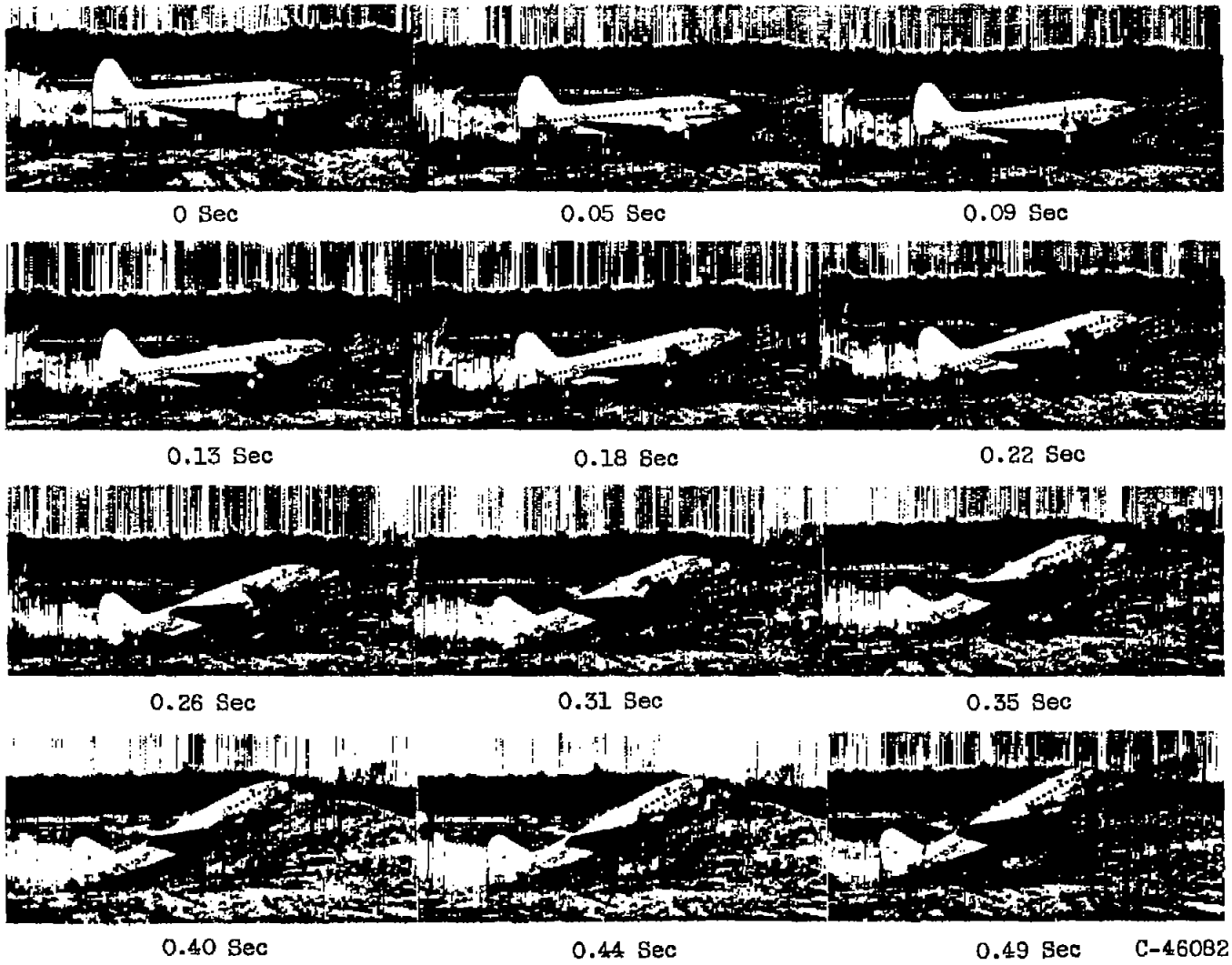

(c) Angle of impact, 29°; impact speed, 97 mph.

Figure 3. - Continued. Sequence pictures and accelerations of crashes of pressurized transports. (Zero time is fuselage nose impact with ground.)

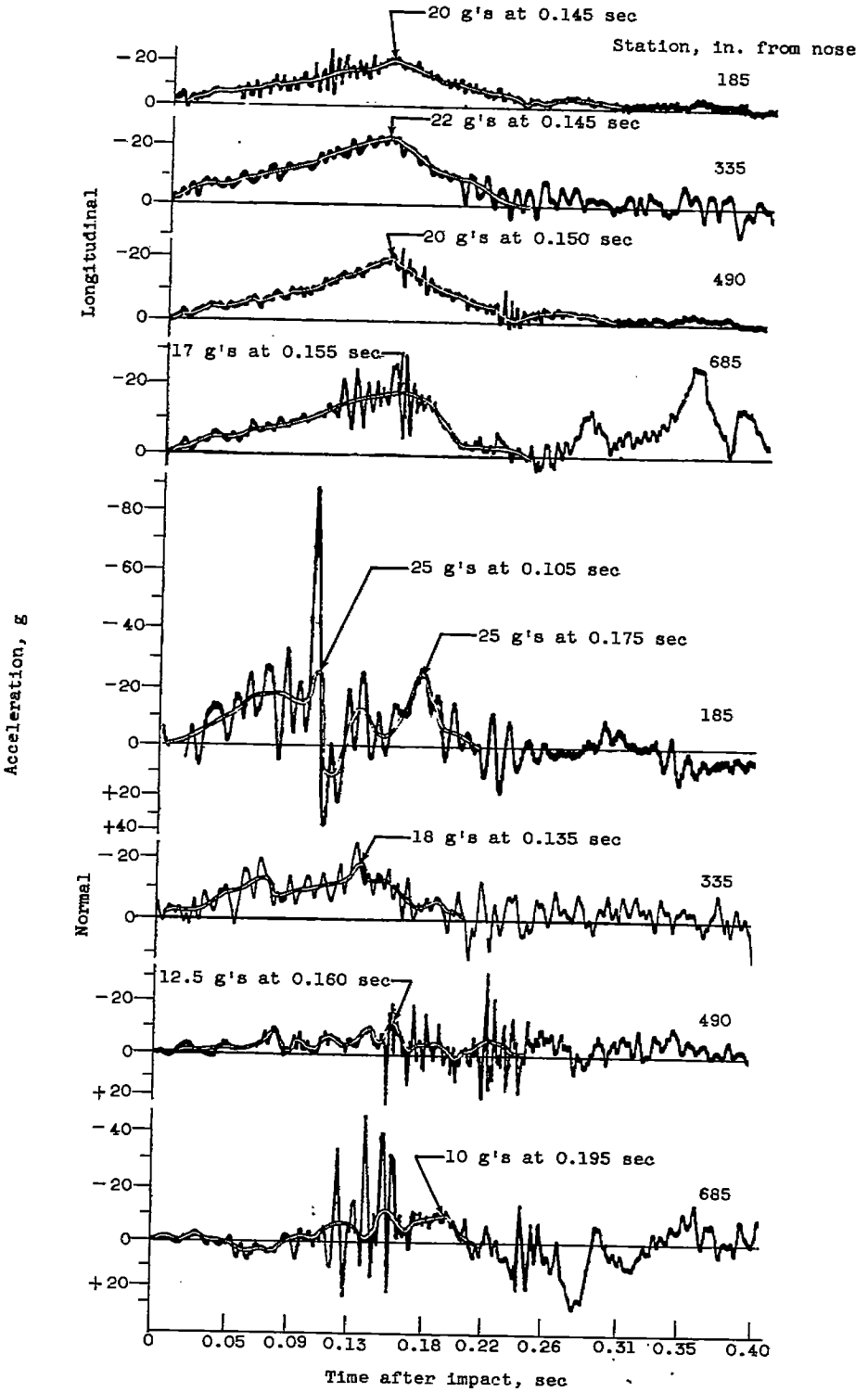

(c) Concluded. Angle of impact, 29°; impact speed, 97 mph.

Figure 3. - Concluded. Sequence pictures and accelerations of crashes of pressurized transports. (Zero time is fuselage nose impact with ground.)

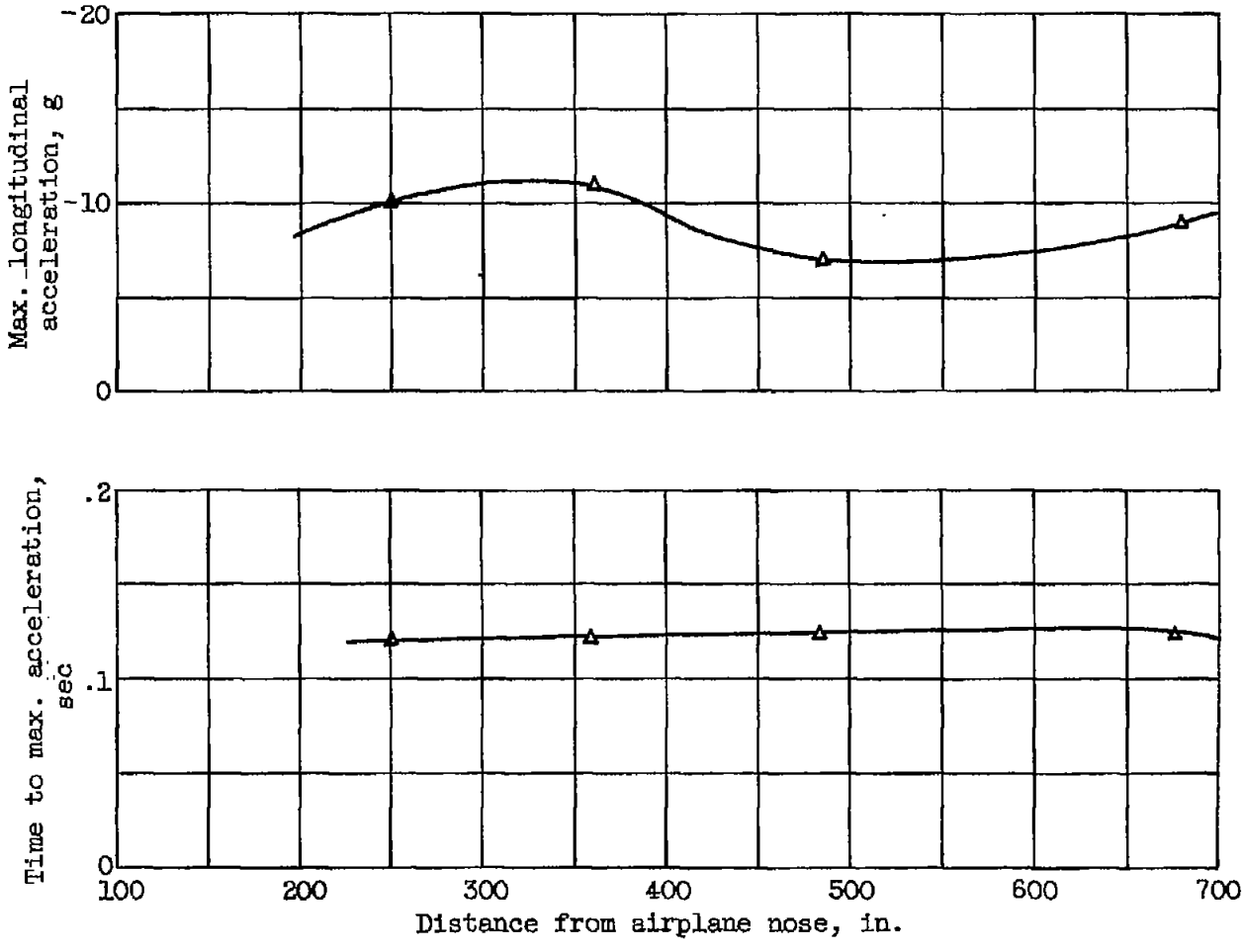

(a) Angle of impact, 15°.

Figure 4. - Variation of maximum longitudinal acceleration and time to reach peak acceleration with position in airplane during crashes of pressurized transports.

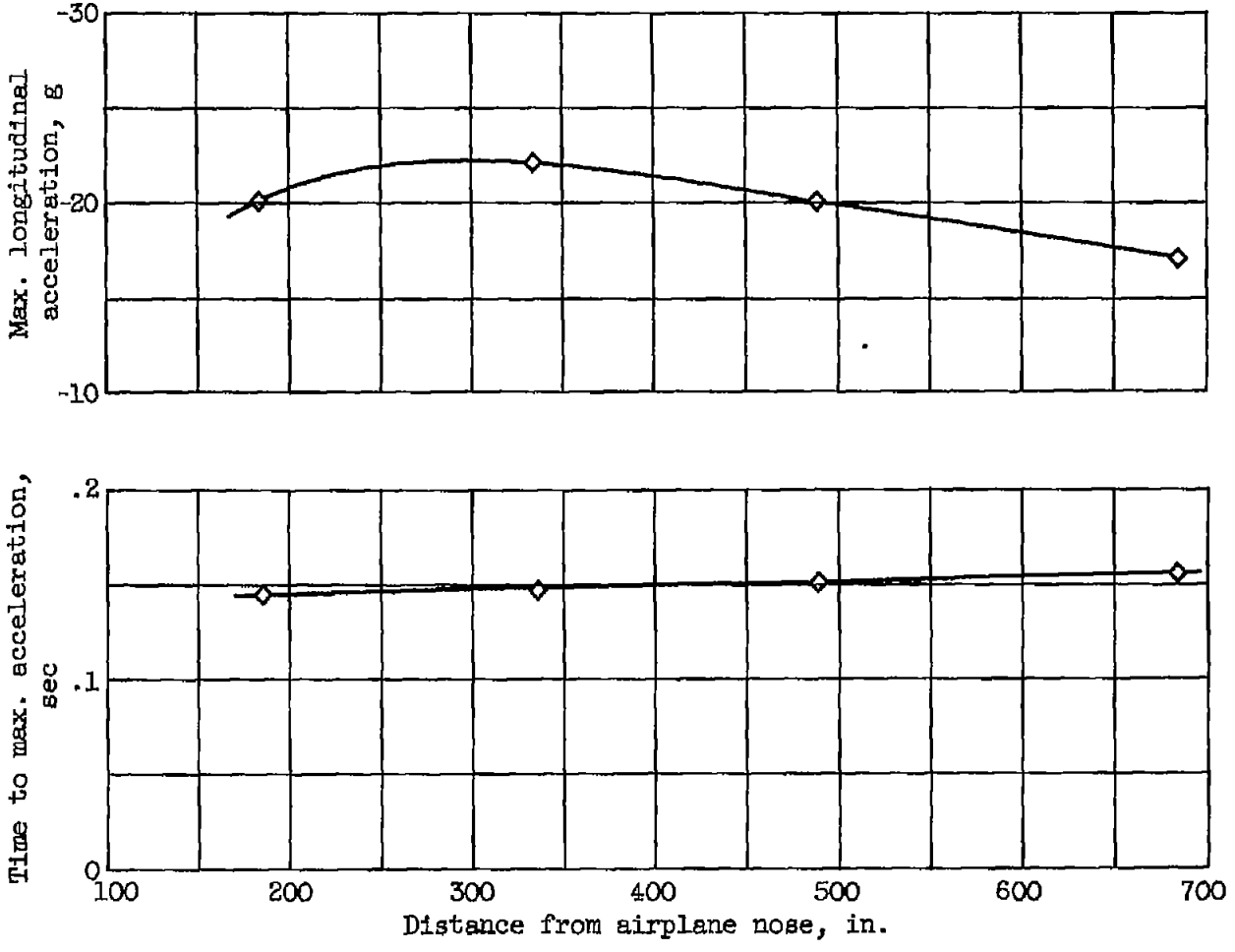

(b) Angle of impact, 29°.

Figure 4. - Concluded. Variation of maximum longitudinal acceleration and time to reach peak acceleration with position in airplane during crashes of pressurized transports.

4462

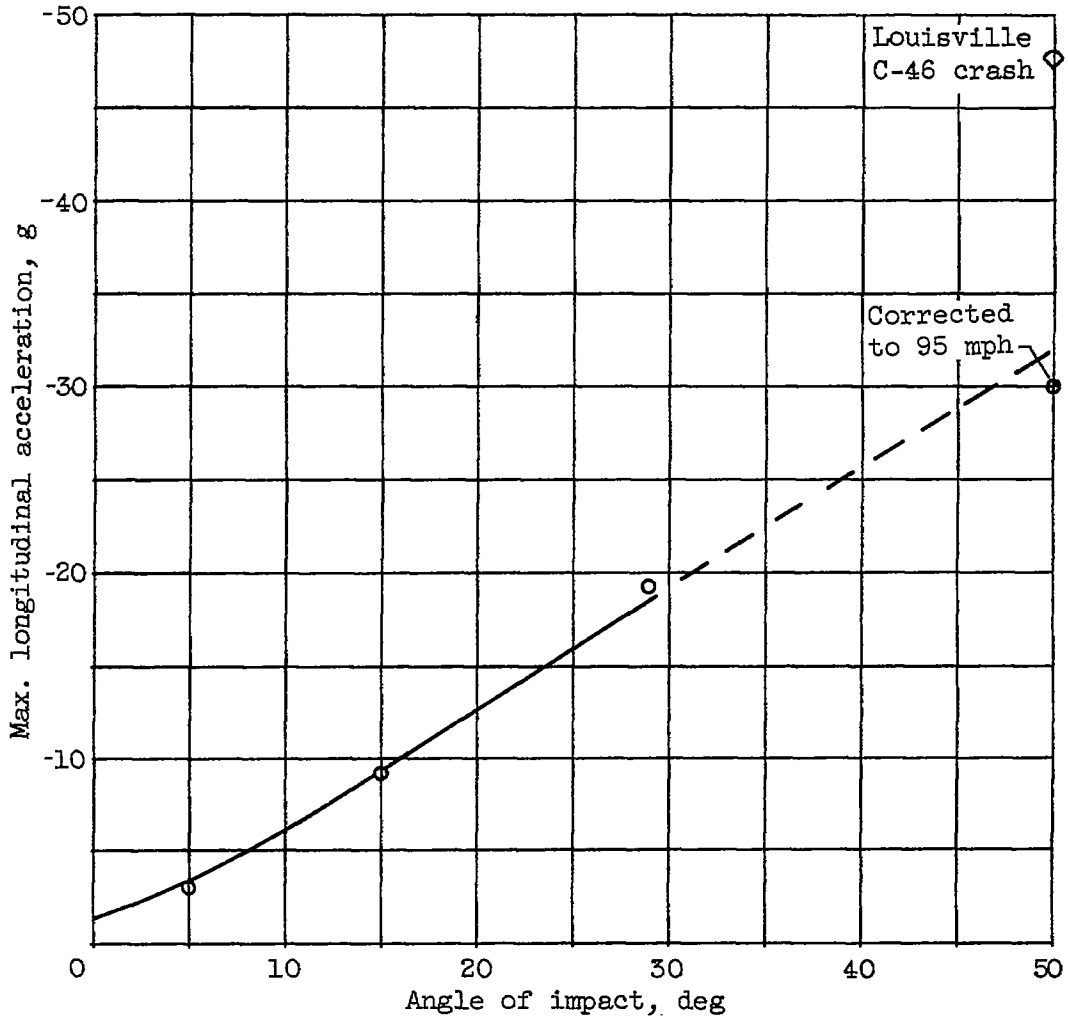

Figure 5. - Variation of maximum longitudinal acceleration with impact angle during crashes of pressurized transports (impact speed corrected to 95 mph).

4462

4462

(a) Side view.

(b) Front view.

Figure 6. - Extent of fuselage crumpling resulting from Louisville crash of pressurized transport at 50° angle of impact and 150 mph.

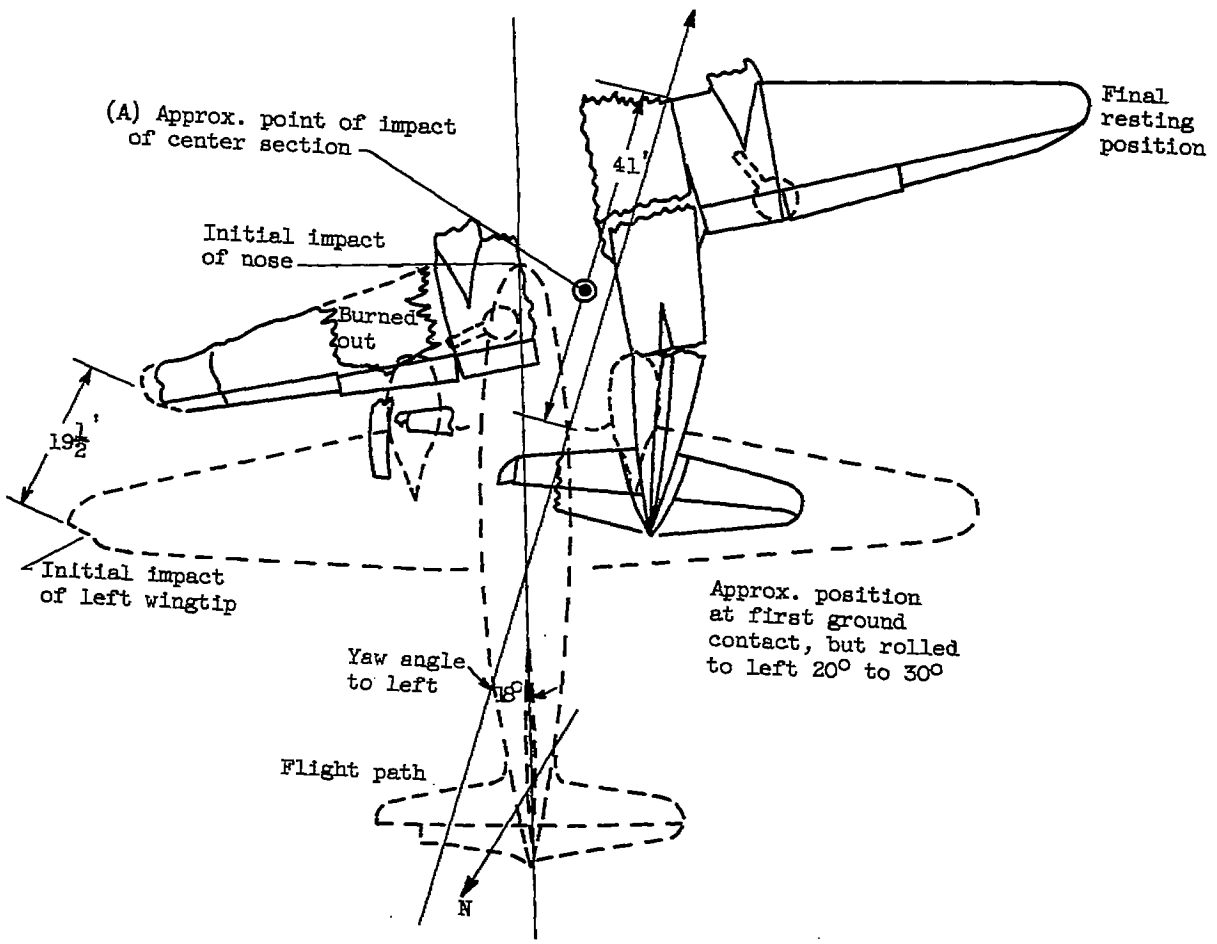

Figure 7. - Distribution of wreckage of C-46 that crashed at Louisville in September 1953.

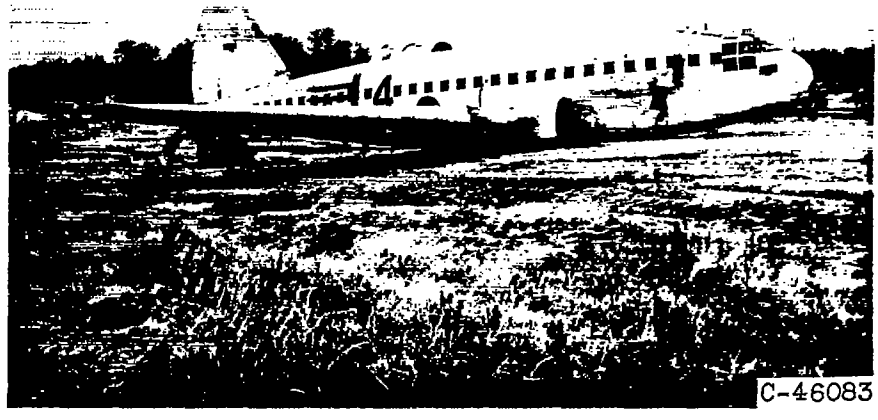

(a) Angle of impact, 5°; impact speed, 81 mph.

Figure 8. - Extent of fuselage crushing resulting from three crashes of pressurized transport airplanes.

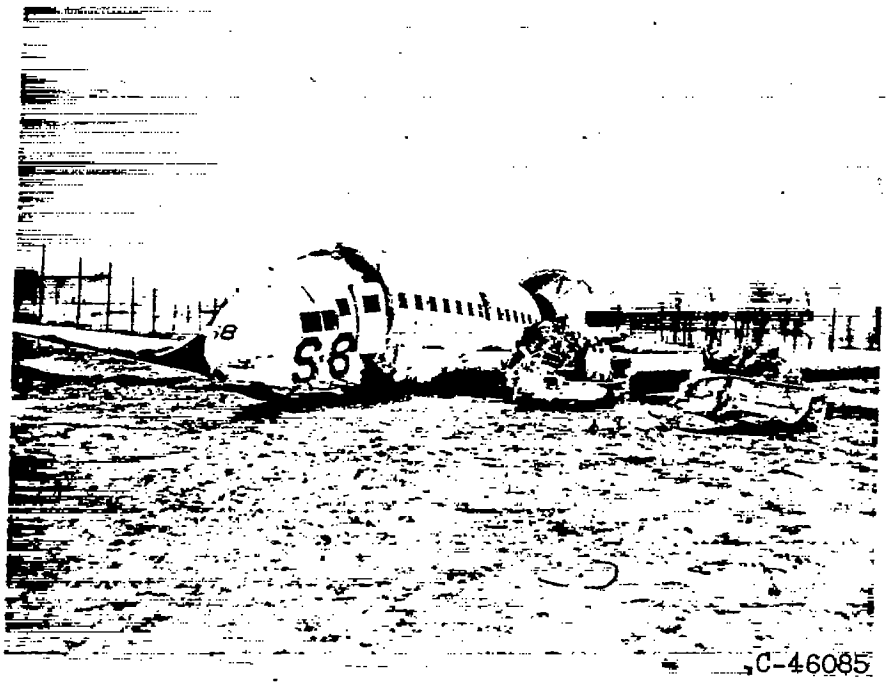

(b) Angle of impact, 15°; impact speed, 93 mph.

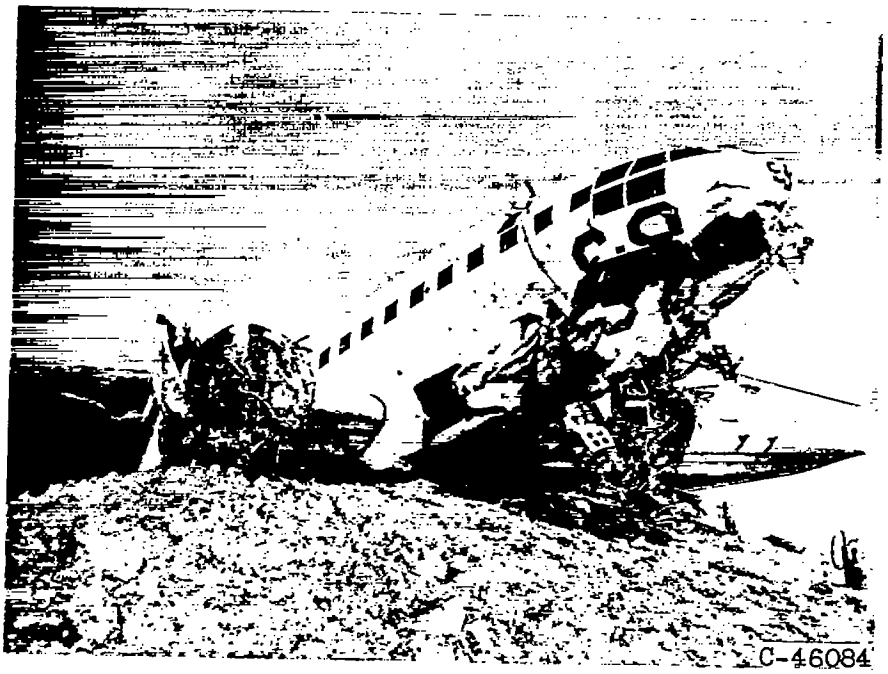

(c) Angle of impact, 29°; impact speed, 97 mph.

Figure 8. - Concluded. Extent of fuselage crushing resulting from three crashes of pressurized transport airplanes.

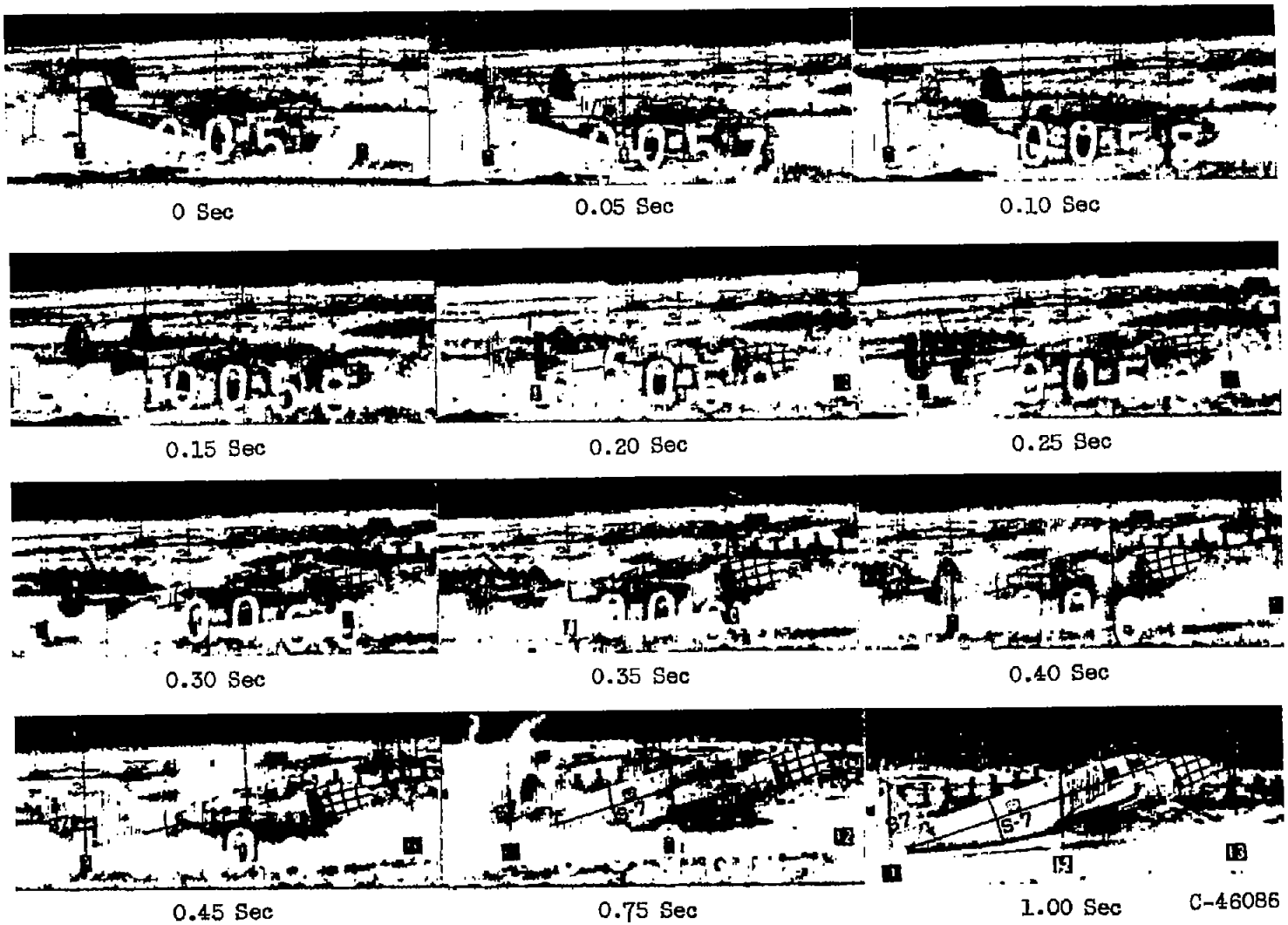

(a) Sequence pictures and accelerations during initial 12° impact. (Zero time corresponds to fuselage impact with ground.)

Figure 9. - Groundloop crash of low-wing unpressurized transport at 12° angle of impact. Impact speed, 87 mph.

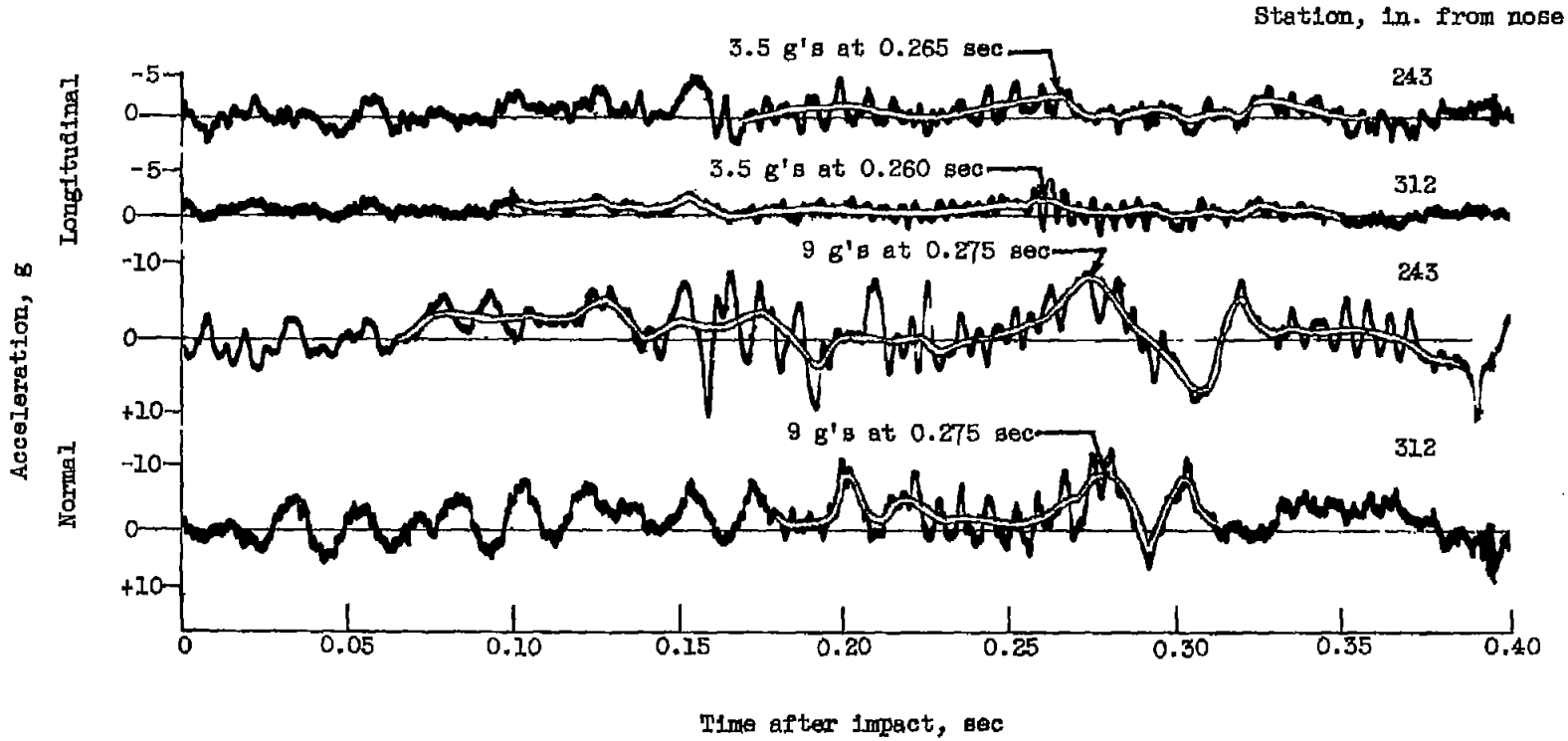

(a) Concluded. Sequence pictures and accelerations during initial 12° impact. (Zero time corresponds to fuselage impact with ground.)

Figure 9. - Continued. Groundloop crash of low-wing unpressurized transport at 12° angle of impact. Impact speed, 87 mph.

4462

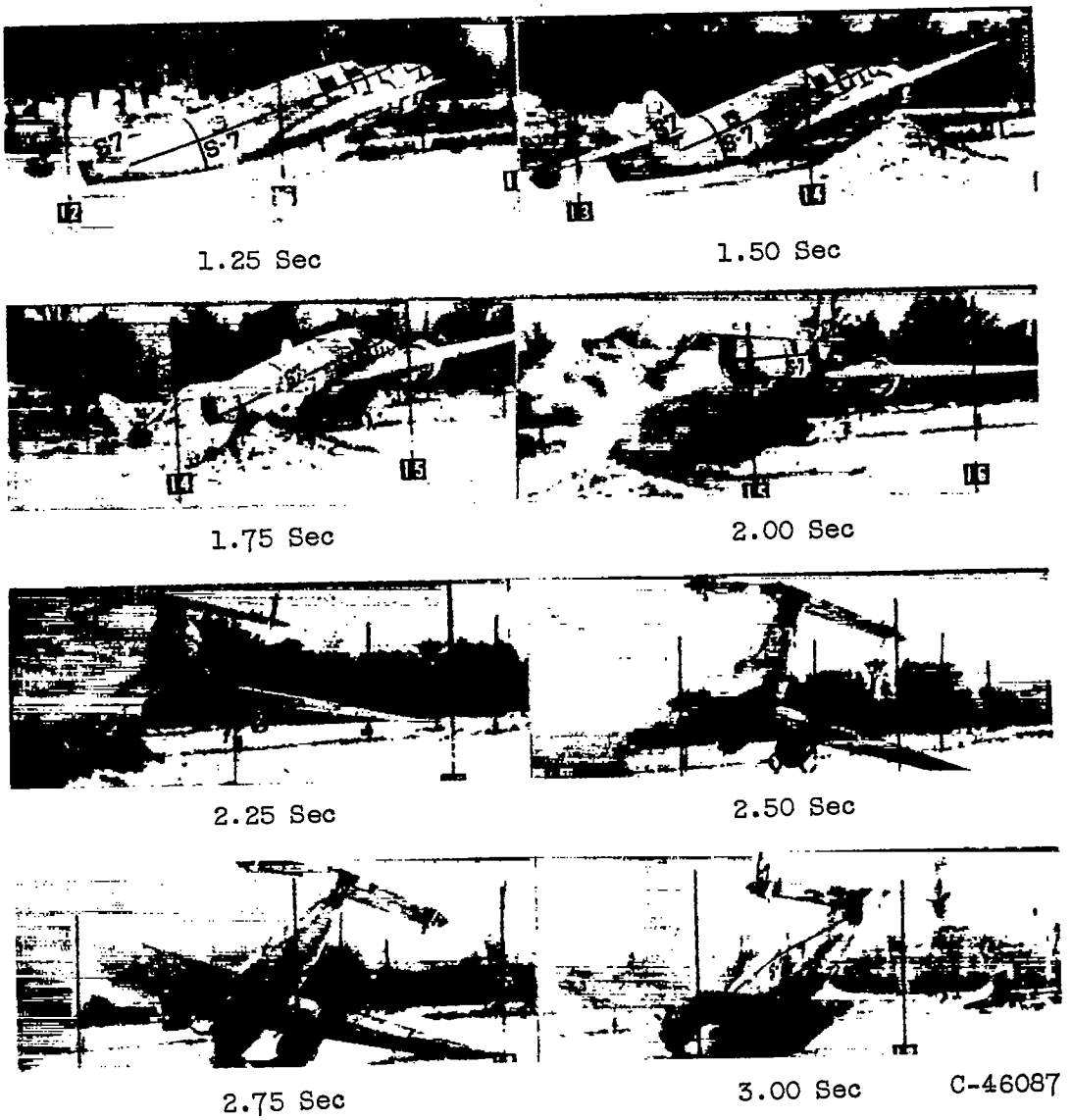

(b) Sequence pictures and accelerations during groundloop.

Figure 9. - Continued. Groundloop crash of low-wing unpressurized transport at 12° angle of impact. Impact speed, 87 mph.

4462

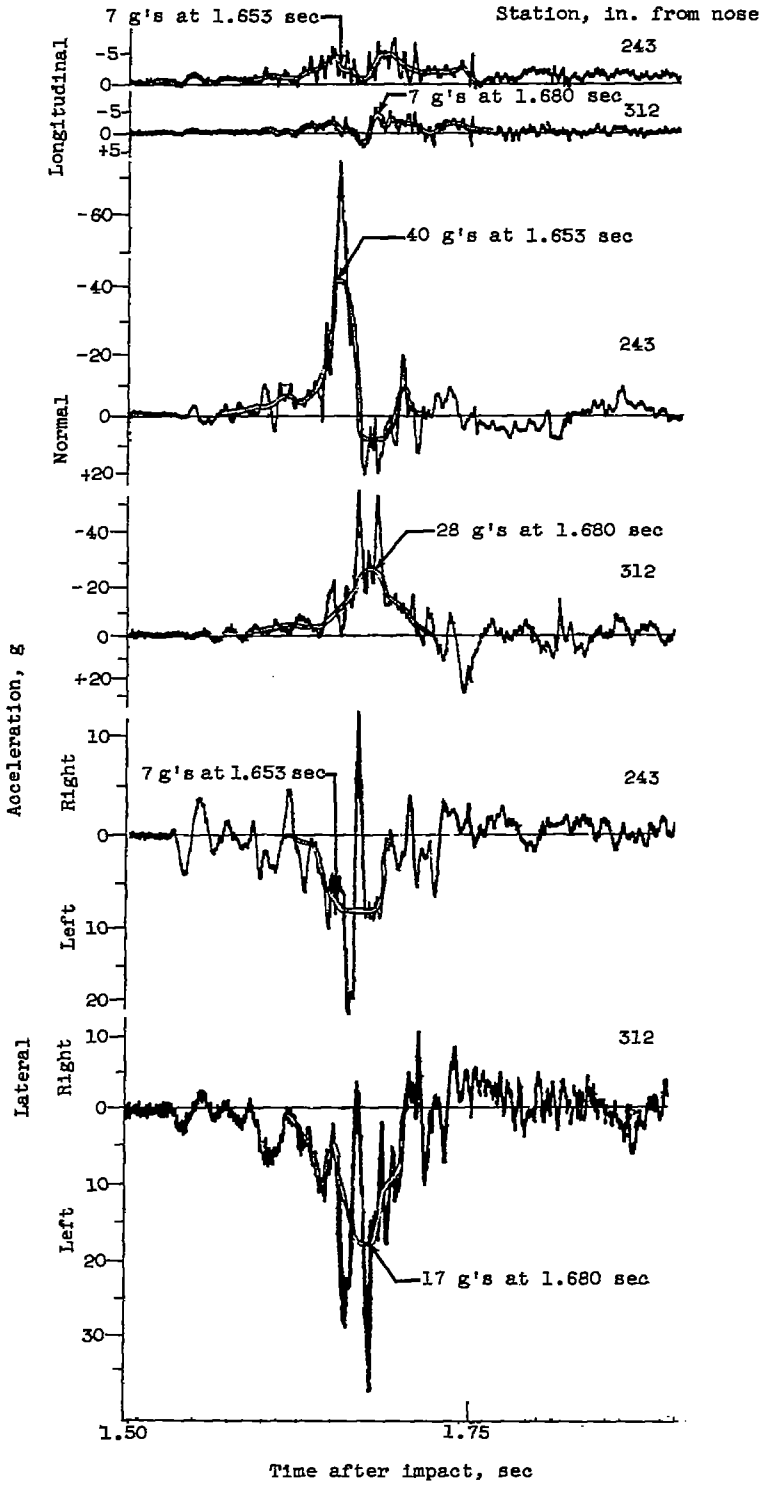

(b) Concluded. Sequence pictures and accelerations during groundloop.

Figure 9. - Continued. Groundloop crash of low-wing unpressurized transport at 12° angle of impact. Impact speed, 87 mph.

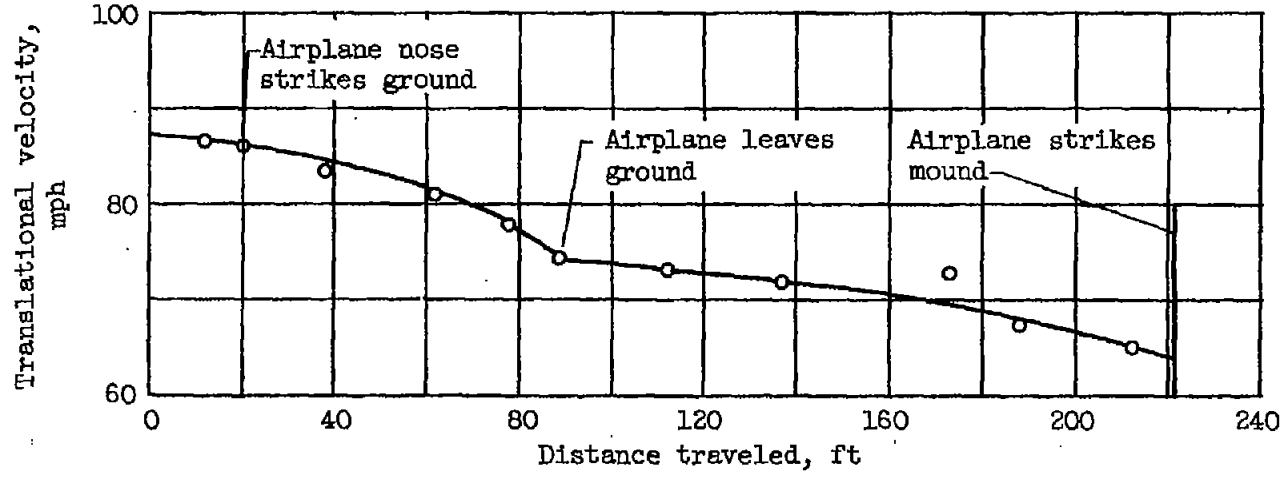

(c) History of translational velocity.

Figure 9. - Concluded. Groundloop crash of low-wing unpressurized transport at 12° angle of impact. Impact speed, 87 mph.

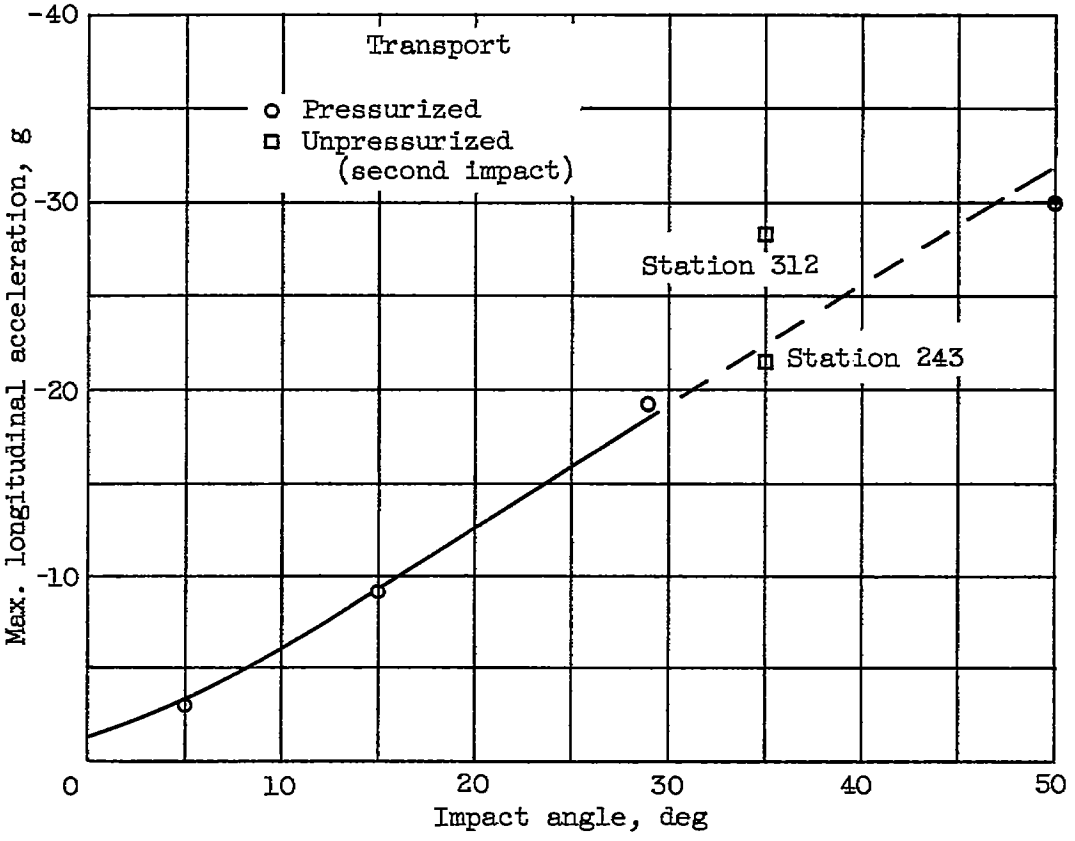

Figure 10. - Variation of maximum longitudinal acceleration with impact angle during crashes of low-wing pressurized and unpressurized transports (impact speed corrected to 95 mph).

4462

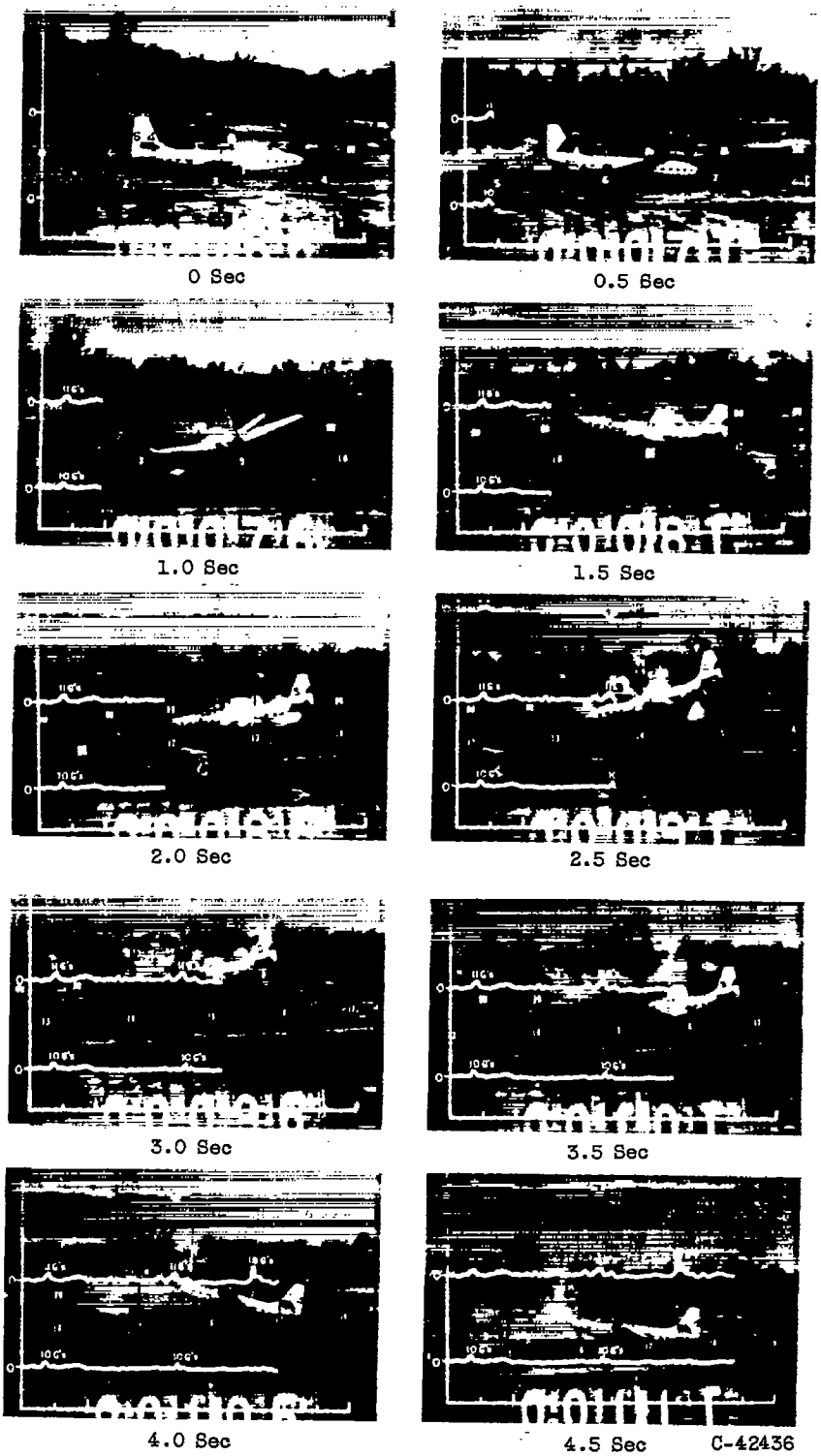

(a) Sequence pictures with superimposed acceleration graphs. Top curve, longitudinal; middle curve, normal; bottom curve, lateral.

Figure 11. - Groundloop crash of FH-1 fighter airplane.

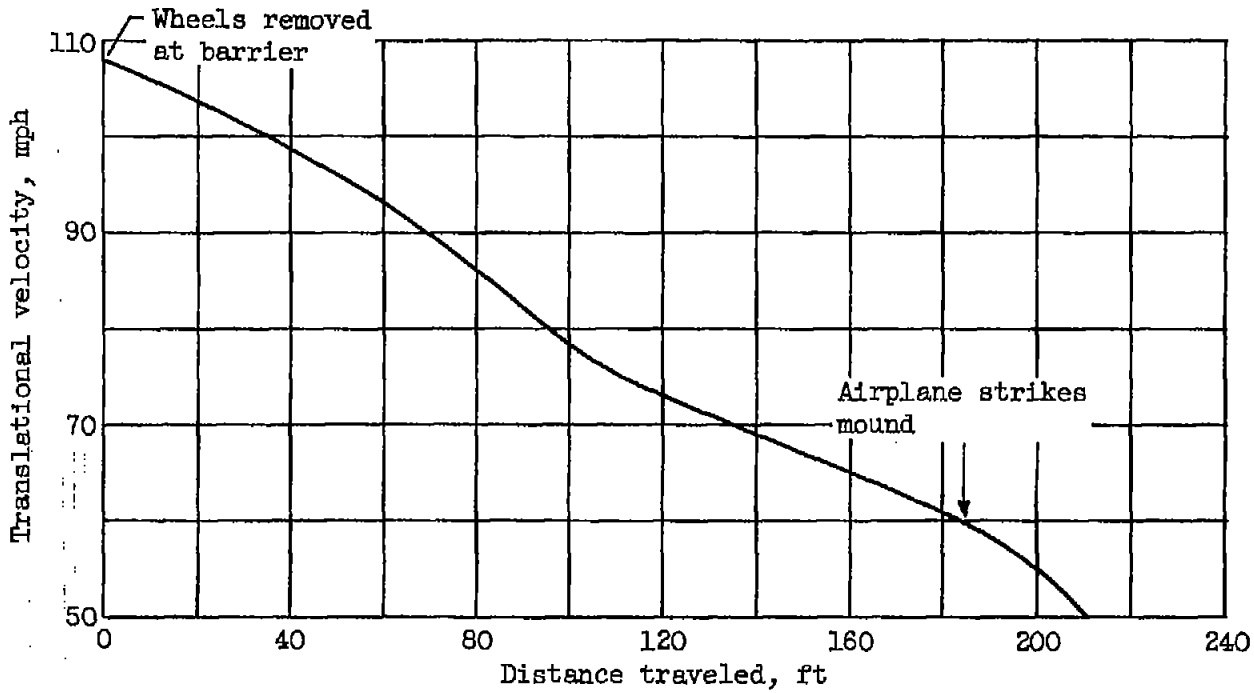

(b) History of translational velocity.

Figure 11. - Concluded. Groundloop crash of FH-1 fighter airplane.

0 Sec 0.63 Sec 1.43 Sec

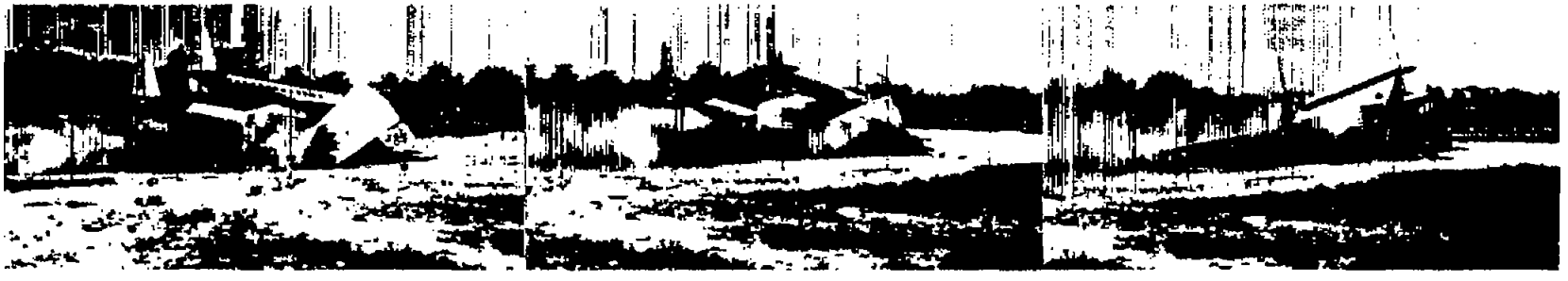

2.21 Sec 3.10 Sec 4.00 Sec

C-46088

4.68 Sec 5.59 Sec

(a) Sequence pictures. (Zero time is propeller impact with wheel barrier.)

Figure 12. - Groundloop crash of high-wing unpressurized transport airplane.

4462

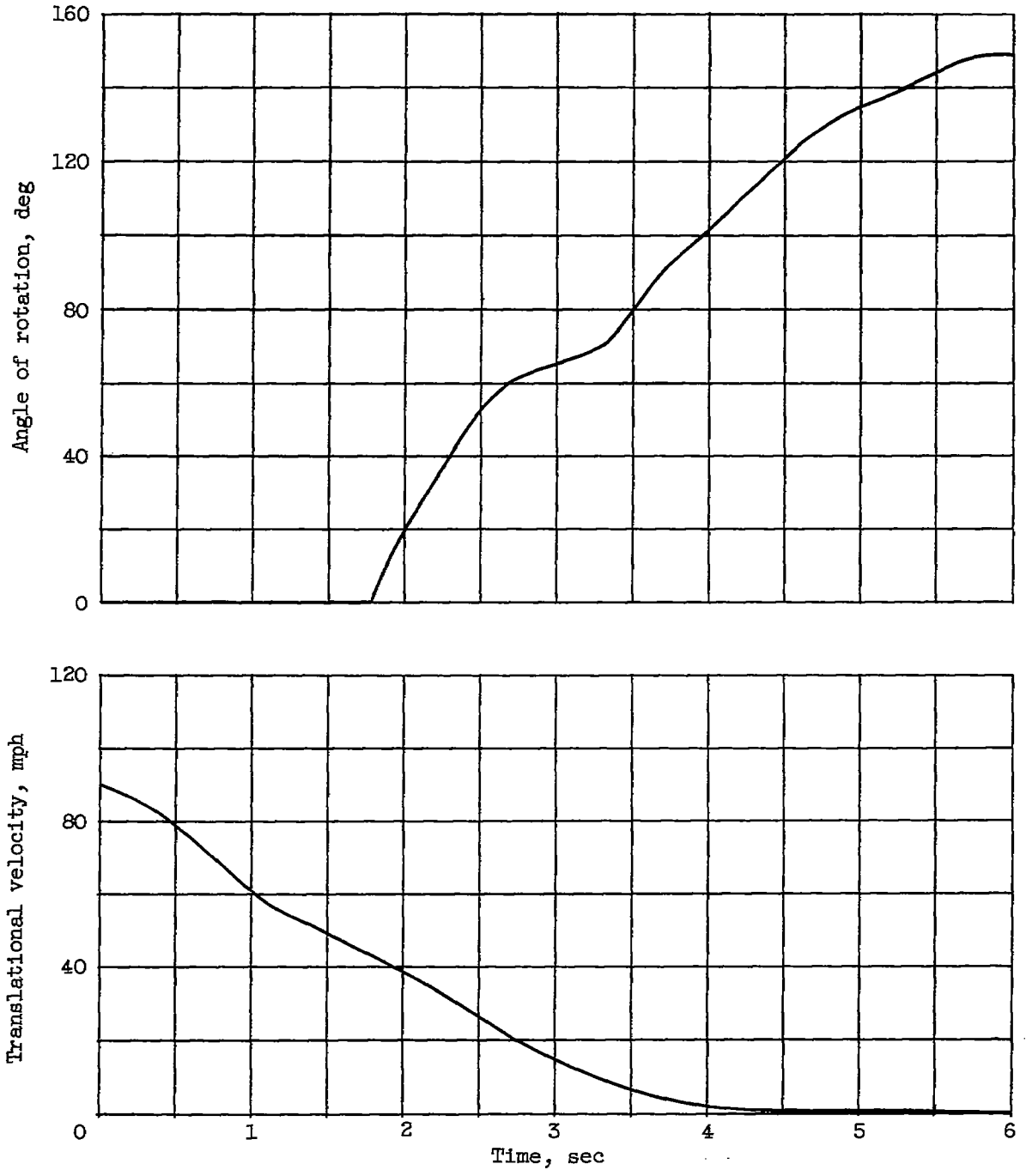

(b) History of translational velocity and angle of rotation.

Figure 12. - Concluded. Groundloop crash of high-wing unpressurized transport airplane.

4462

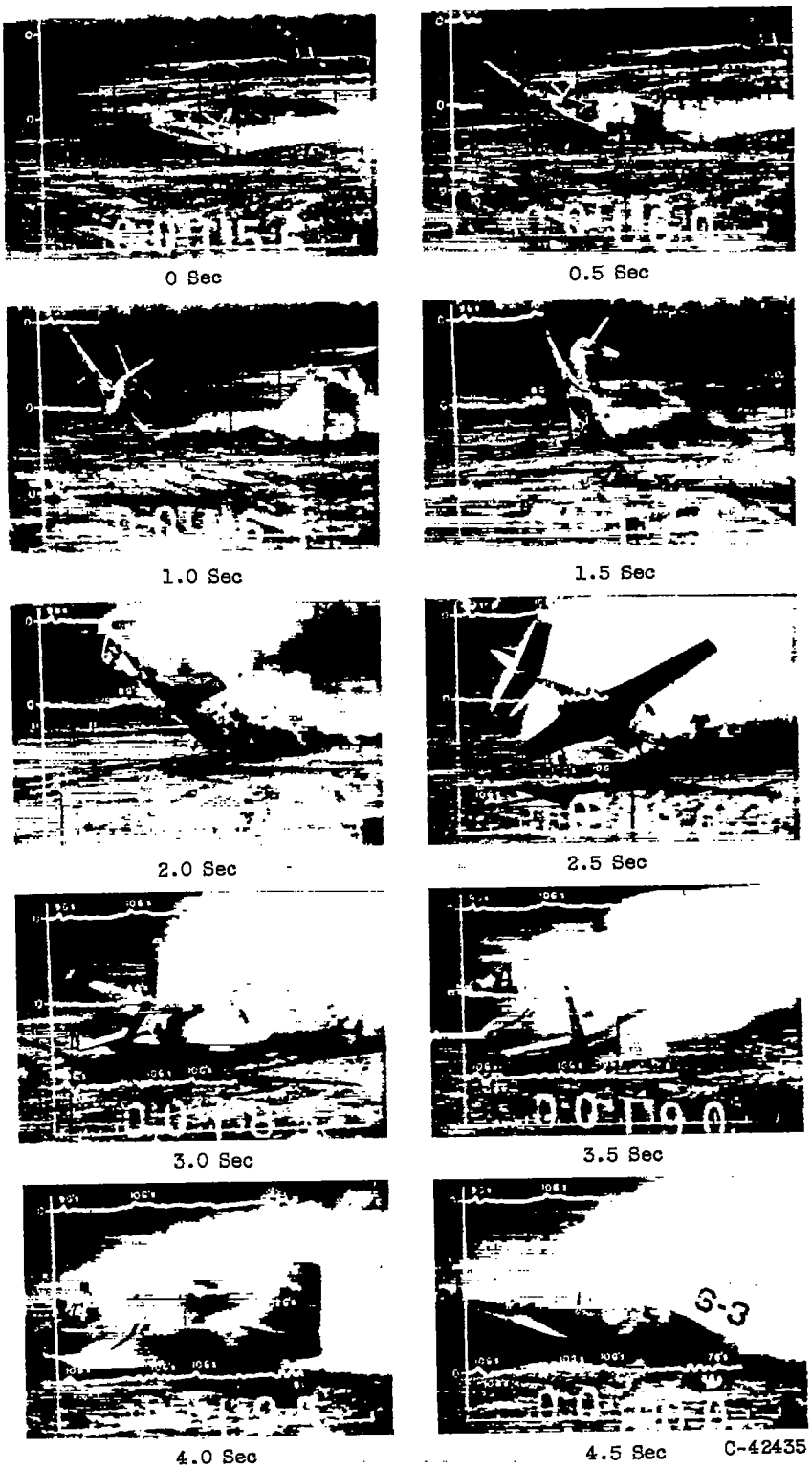

Figure 13. - Sequence pictures of cartwheel crash of FH-1 fighter airplane with superimposed acceleration graphs. Top curve, longitudinal; middle curve, normal; bottom curve, lateral.

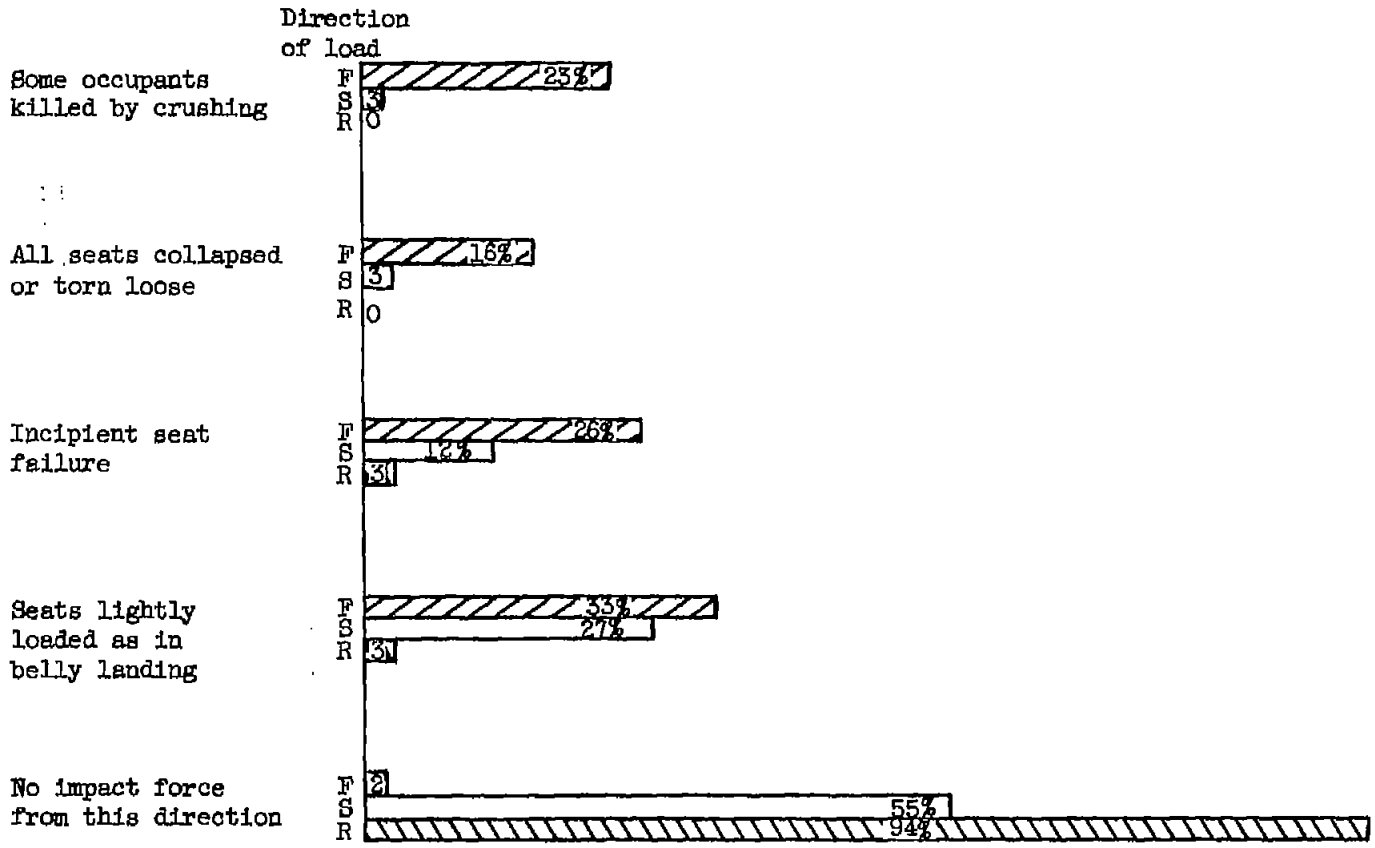

Figure 14. - Analysis of direction of loads in aircraft accidents. (F = front; S = side; R = rear.)

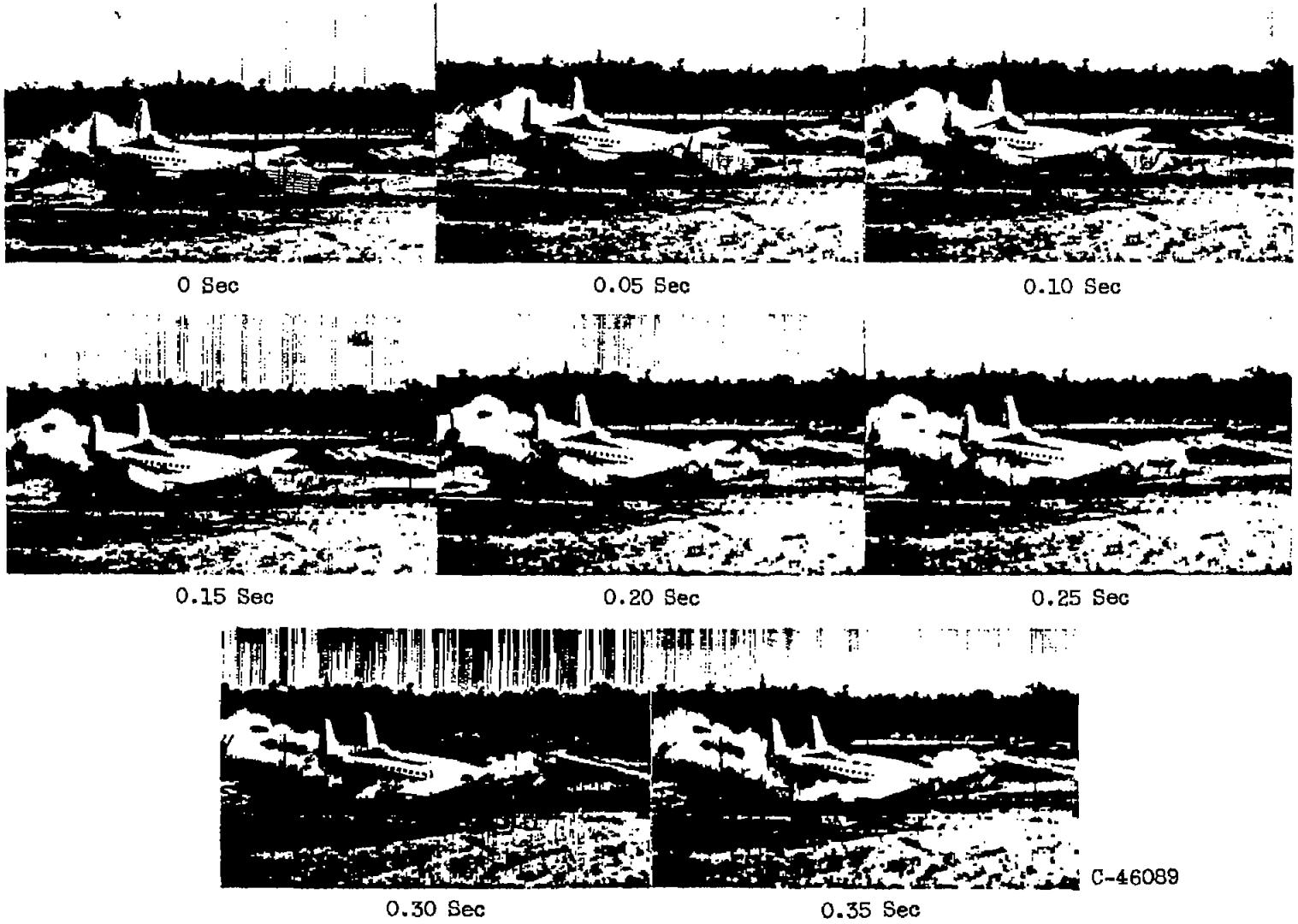

(a) Sequence pictures and accelerations of 16° crash of high-wing airplane. Impact speed, 91 mph.

Figure 15. - Comparison of 16° crashes of high- and low-wing unpressurized transports. (Zero time corresponds to fuselage impact with ground.)

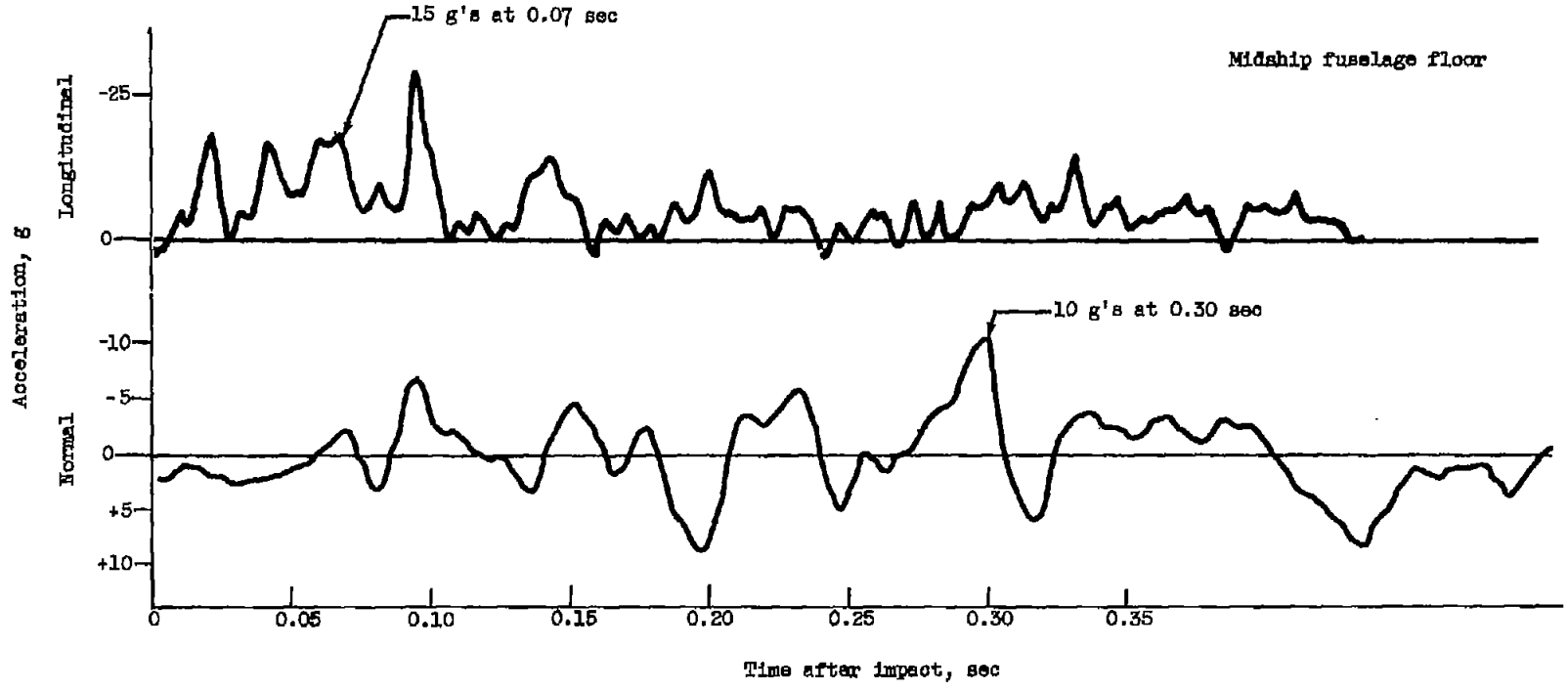

(a) Concluded. Sequence pictures and accelerations of 16° crash of high-wing airplane. Impact speed, 91 mph.

Figure 15. - Continued. Comparison of 16° crashes of high- and low-wing unpressurized transports. (Zero time corresponds to fuselage impact with ground.)

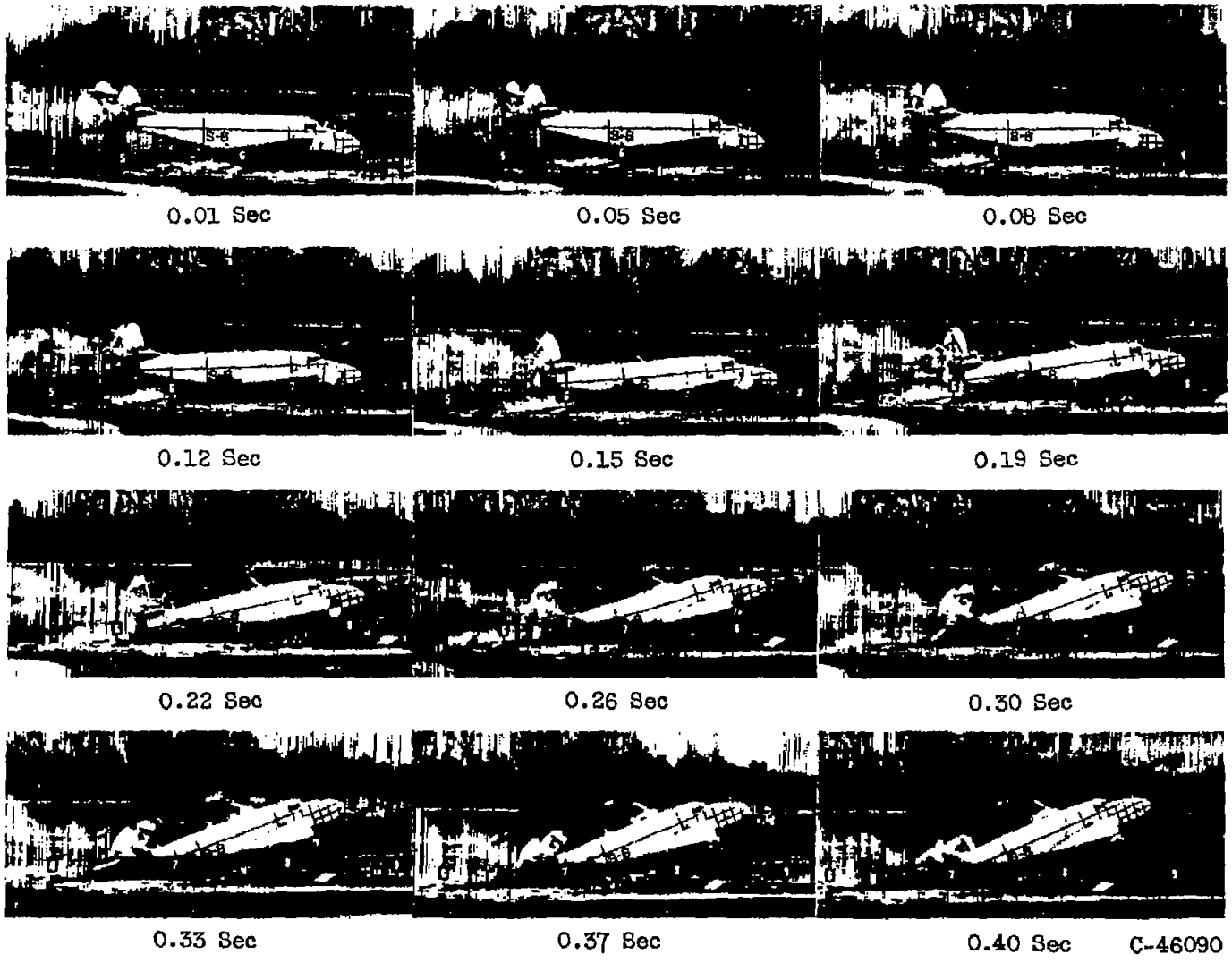

(b) Sequence pictures and accelerations of 16° crash of low-wing airplane. Impact speed, 109 mph.

Figure 15. - Continued. Comparison of 16° crashes of high- and low-wing unpressurized transports. (Zero time corresponds to fuselage impact with ground.)

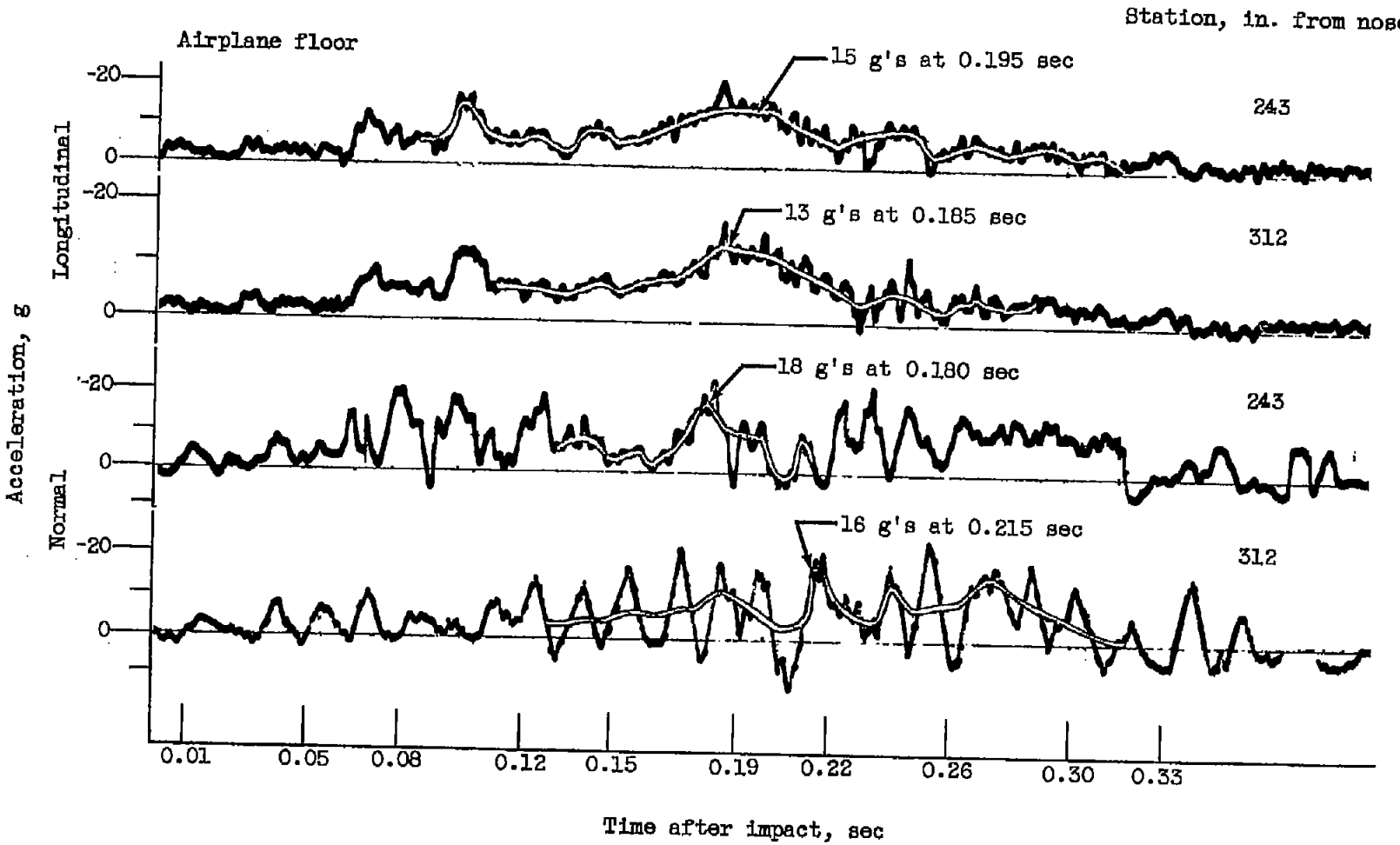

(b) Concluded. Sequence pictures and accelerations of 16° crash of low-wing airplane. Impact speed, 109 mph.

Figure 15. - Continued. Comparison of 16° crashes of high- and low-wing unpressurized transports. (Zero time corresponds to fuselage impact with ground.)

4462

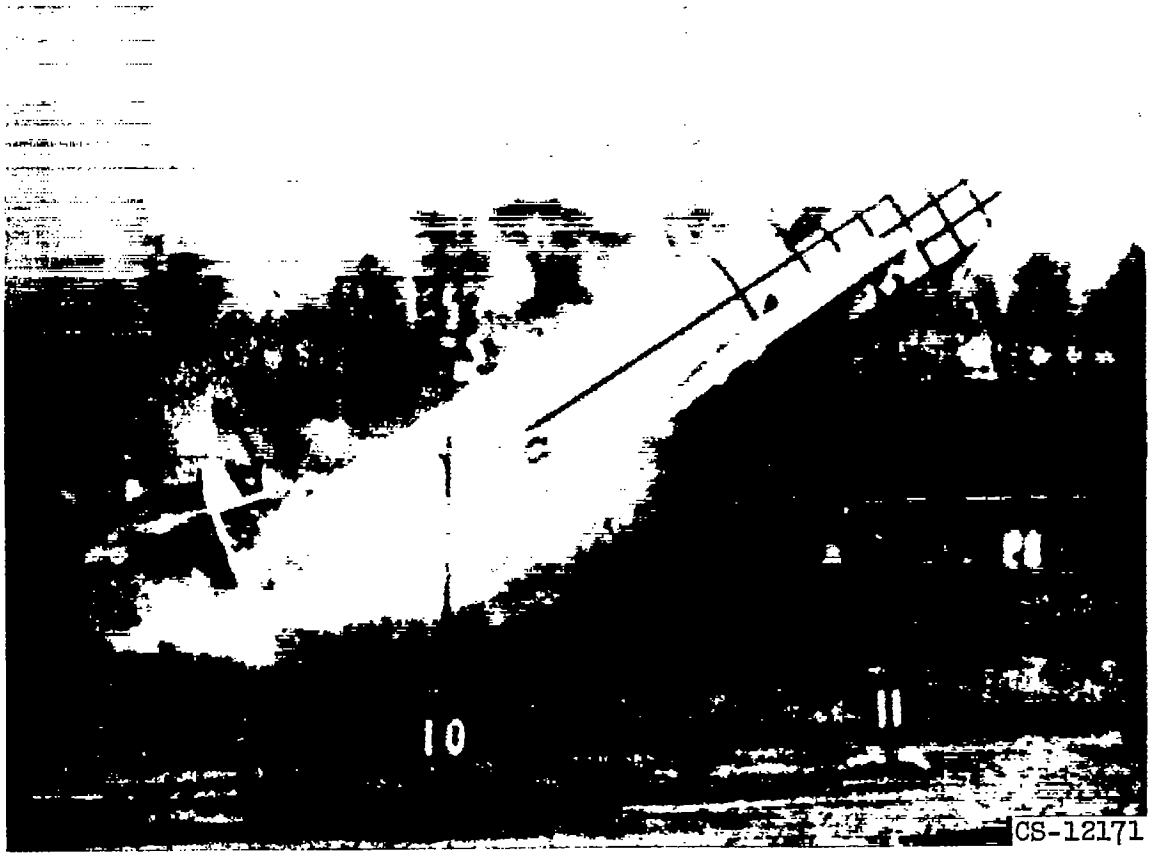

(c) Extent of fuselage crumpling resulting from 16° crash of low-wing airplane.

Figure 15. - Concluded. Comparison of 16° crashes of high- and low-wing unpressurized transports. (Zero time corresponds to fuselage impact with ground.)

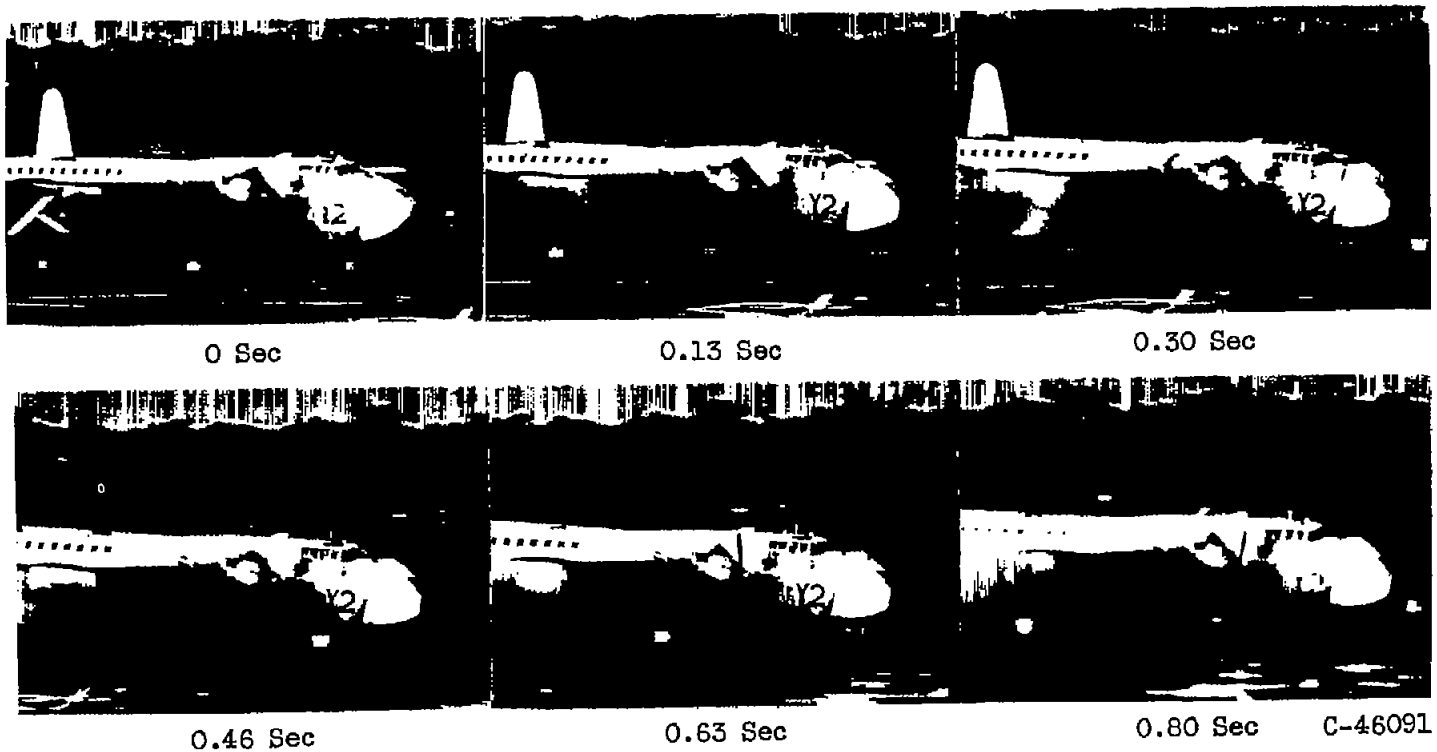

(a) Sequence pictures.

Figure 16. - Sequence pictures and accelerations of 4° crash of high-wing unpressurized transport. Impact speed, 95 mph. (Zero time is fuselage nose impact with ground.)

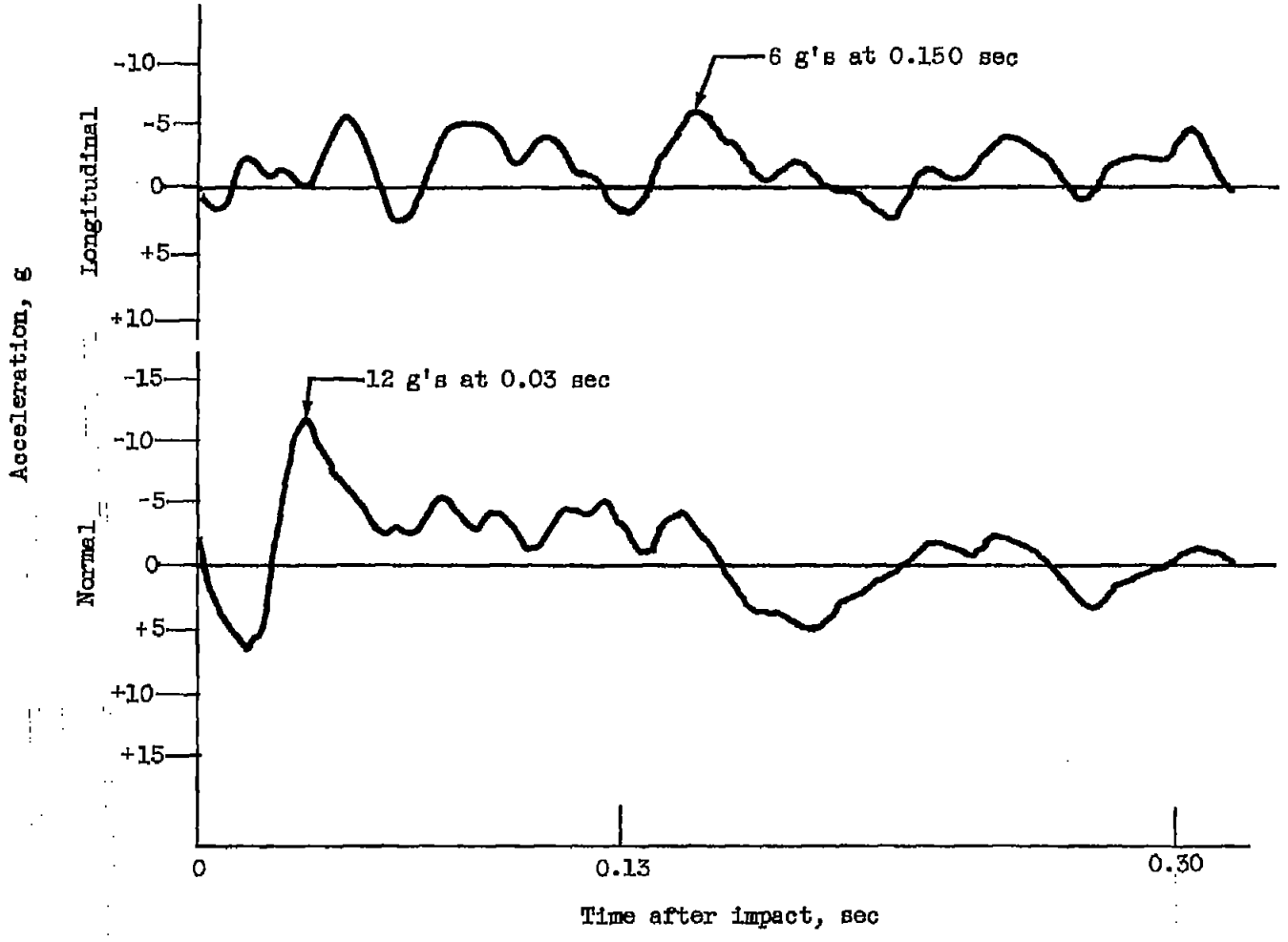

(b) Accelerations.

Figure 16. - Concluded. Sequence pictures and accelerations of 4° crash of high-wing unpressurized transport. Impact speed, 95 mph. (Zero time is fuselage nose impact with ground.)

4462

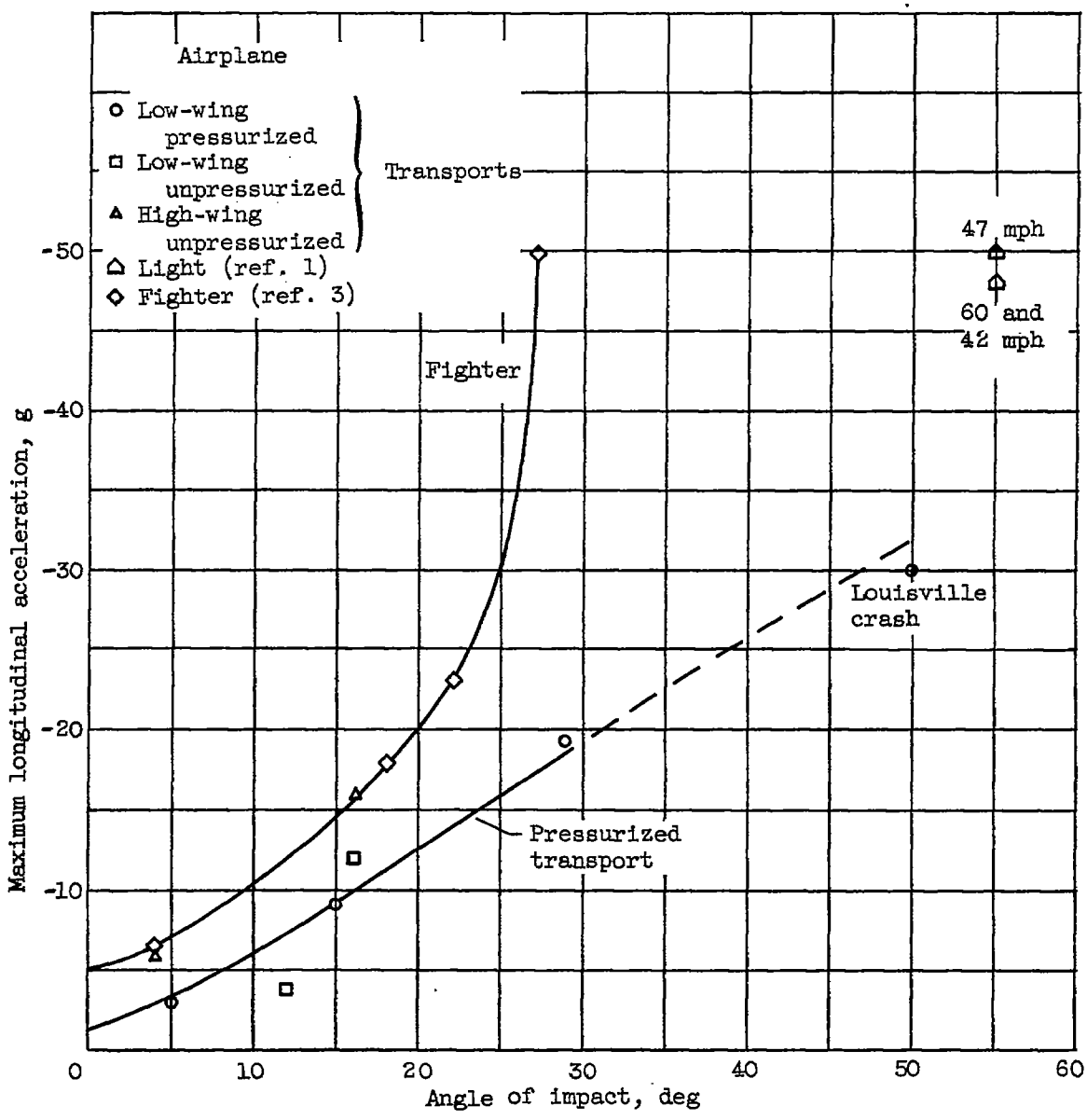

Figure 17. - Effect of airplane configuration on variation of maximum longitudinal acceleration or with impact angle (all impact speeds corrected to 95 mph).

4462

A-VA

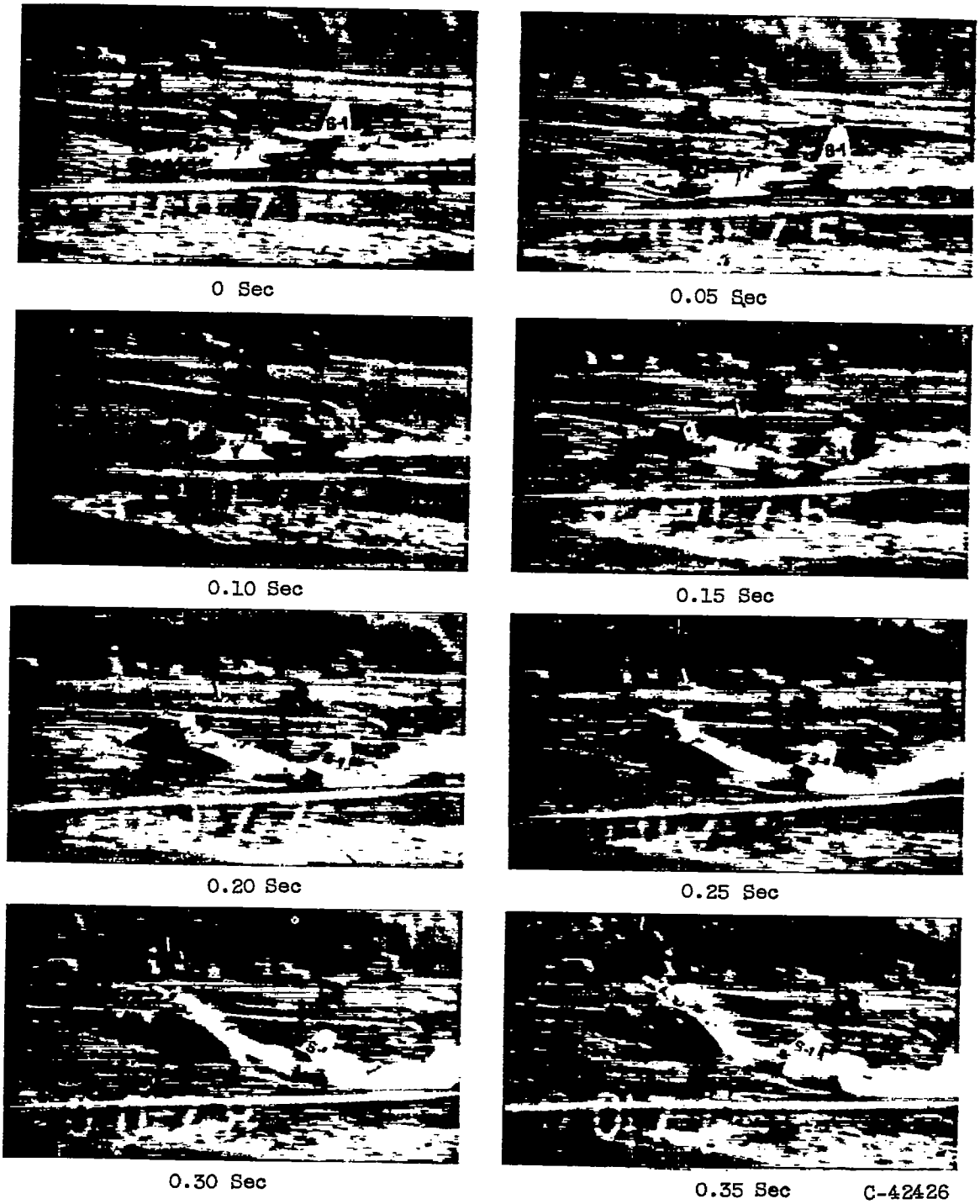

(a) Angle of impact, 18°.

Figure 18. - Sequence pictures of crashes of FH-1 fighter airplanes.

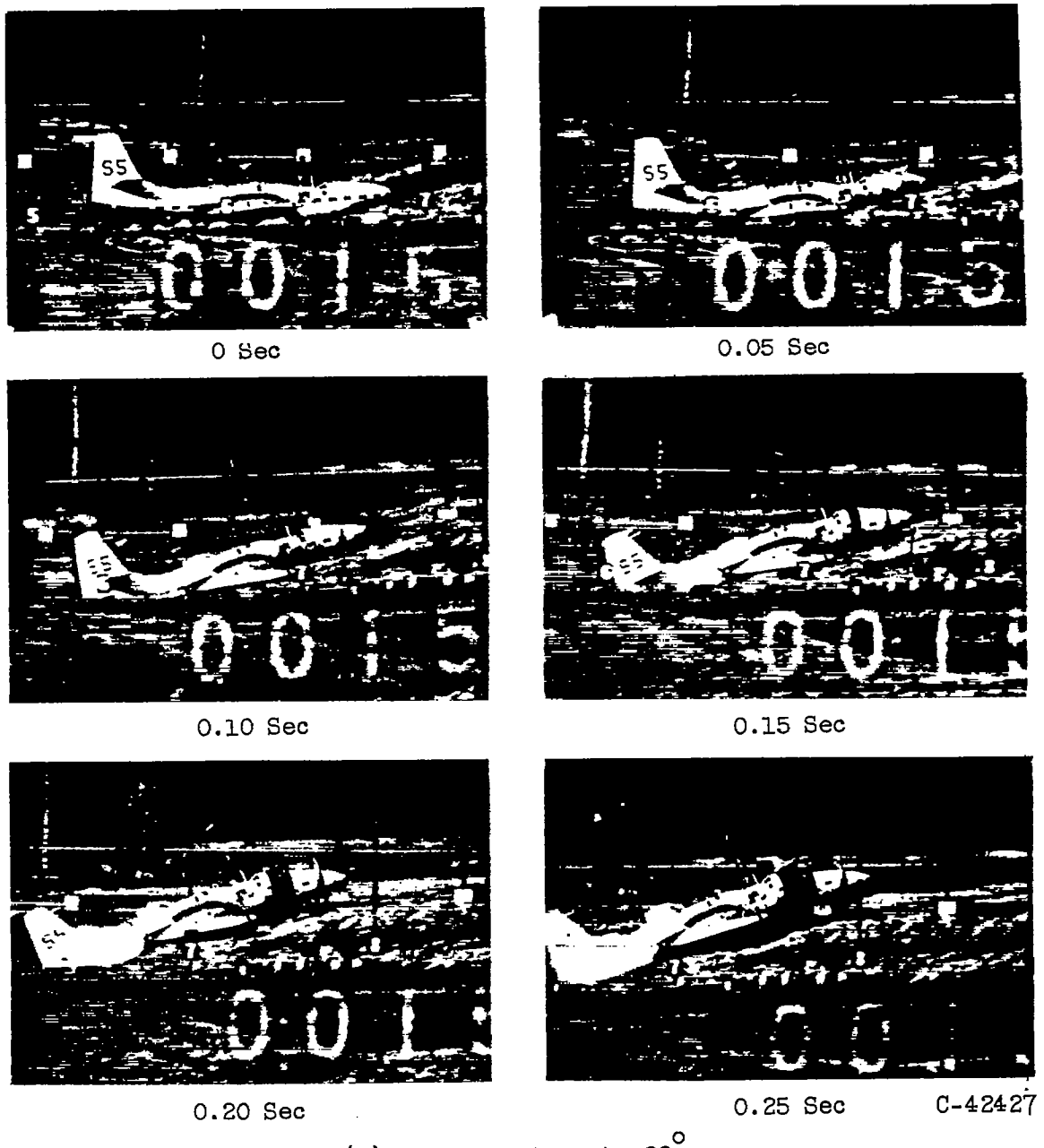

(b) Angle of impact, 22°.

Figure 18. - Continued. Sequence pictures of crashes of FH-1 fighter airplanes.

4462

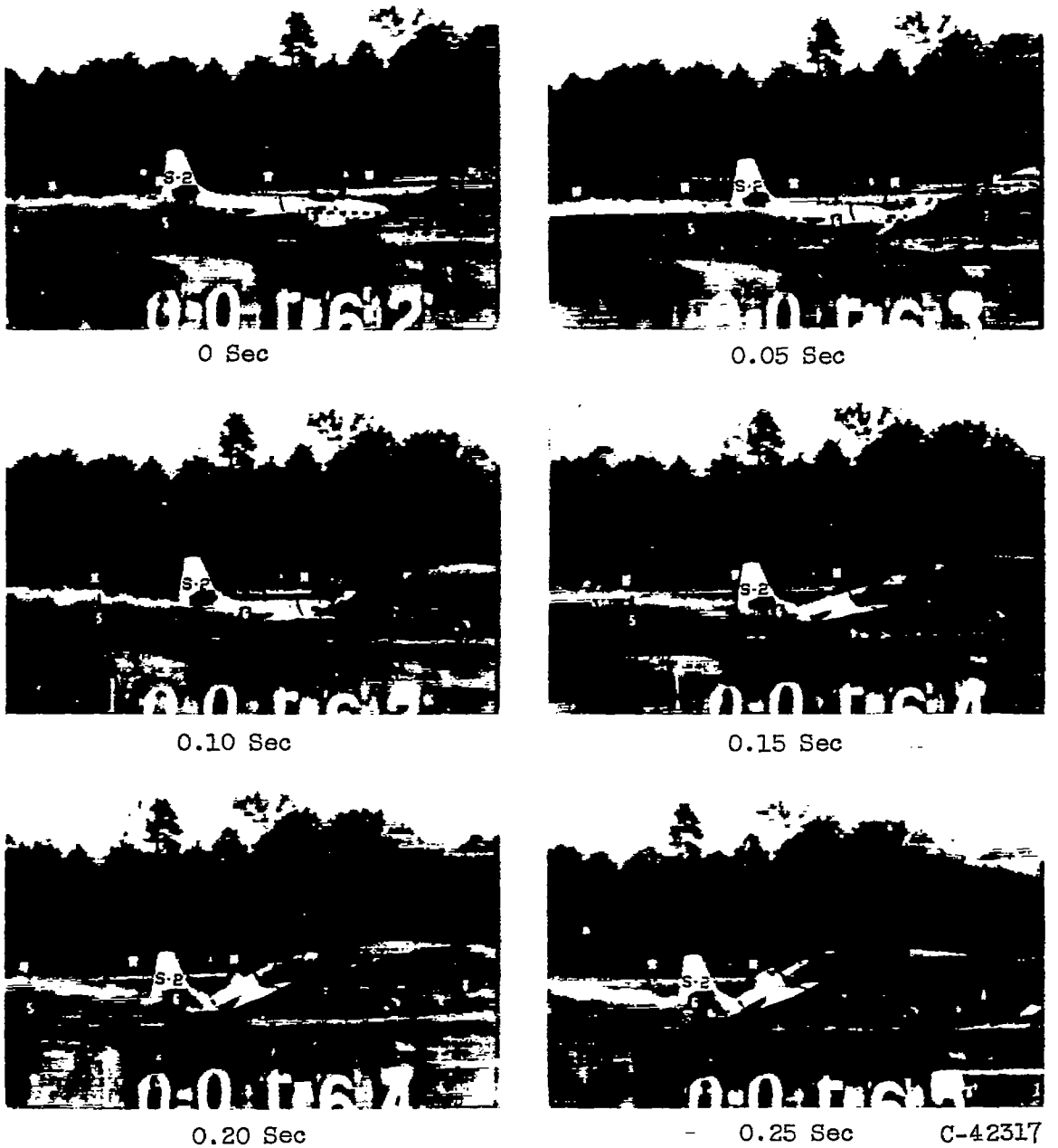

(c) Angle of impact, 27°.

Figure 18. - Concluded. Sequence pictures of crashes of FH-1 fighter airplanes.

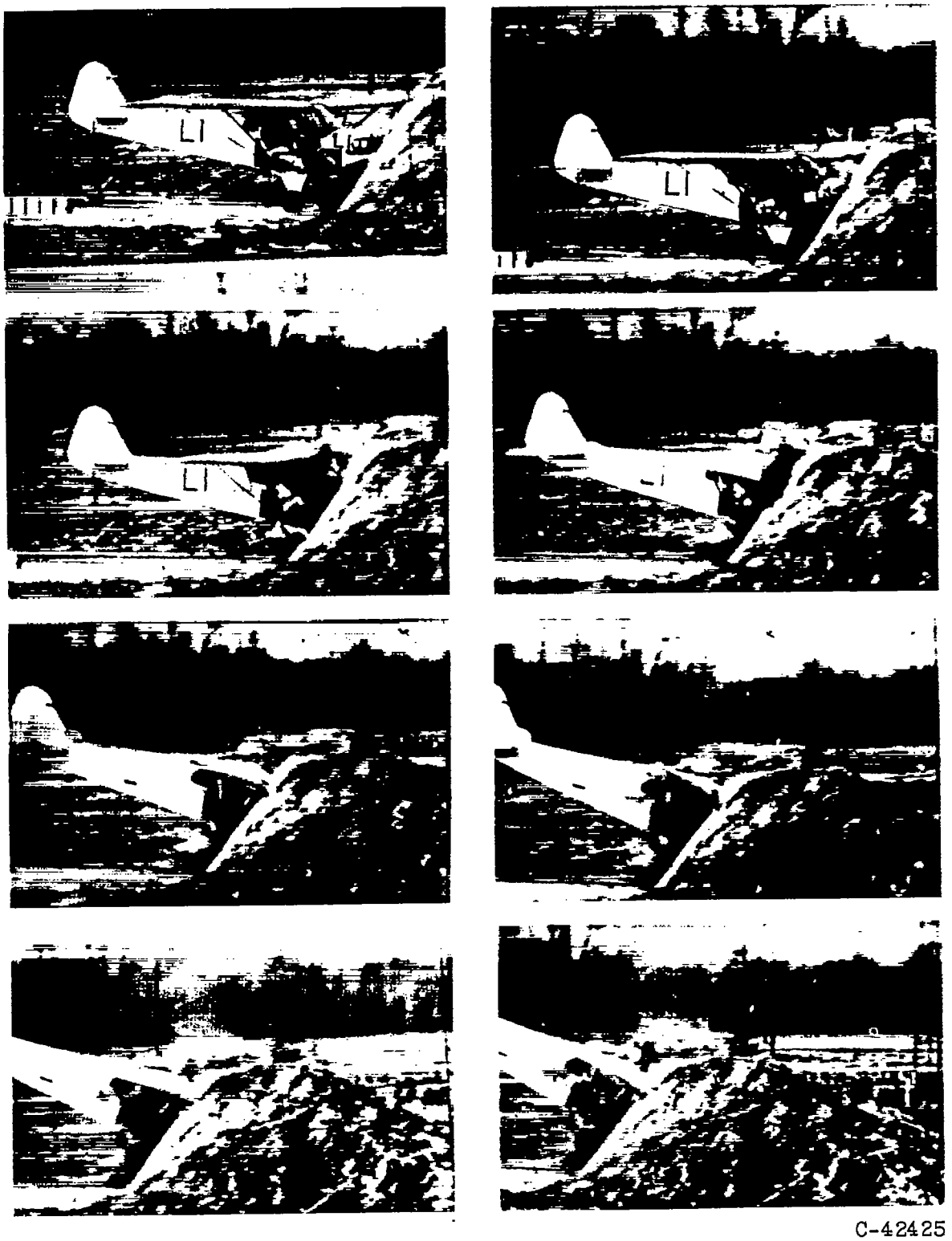

C-42425

Figure 19. - Sequence pictures of 55° crash of light airplane. Impact speed, 60 mph.

4462

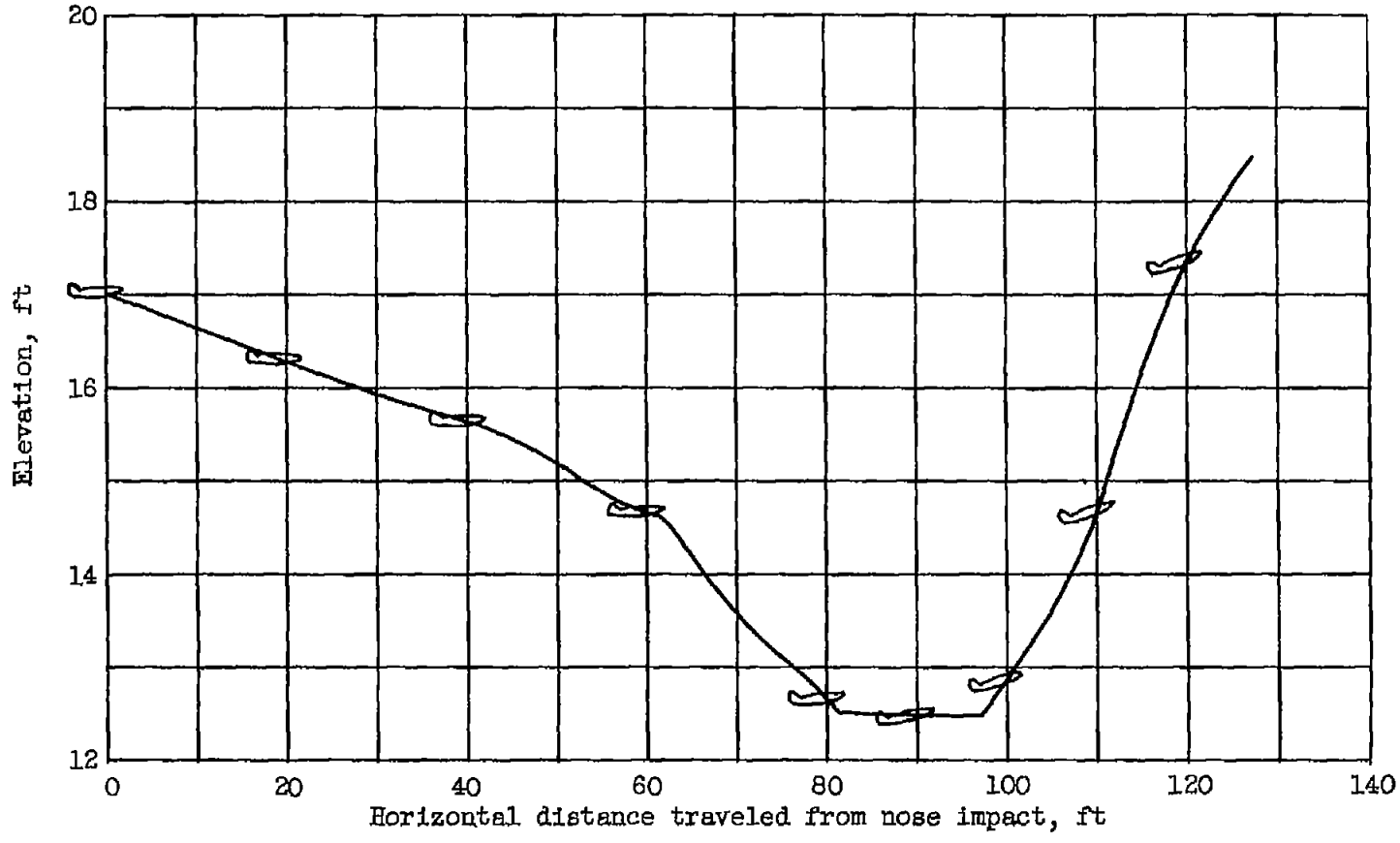

Figure 20. - Trajectory of point on aft part of fuselage and angle of longitudinal axis of airplane to horizontal during crash of pressurized airplane at 15° angle of impact.

4462

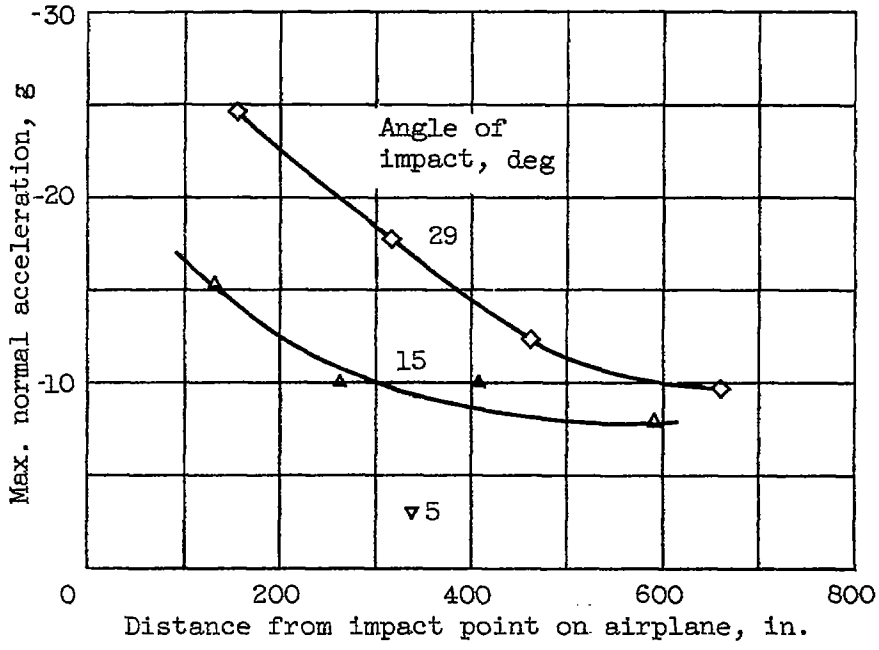

Figure 21. - Variation of maximum normal acceleration with distance from impact point for 5°, 15°, and 29° crashes of pressurized transports (impact speed corrected to 95 mph).

4462

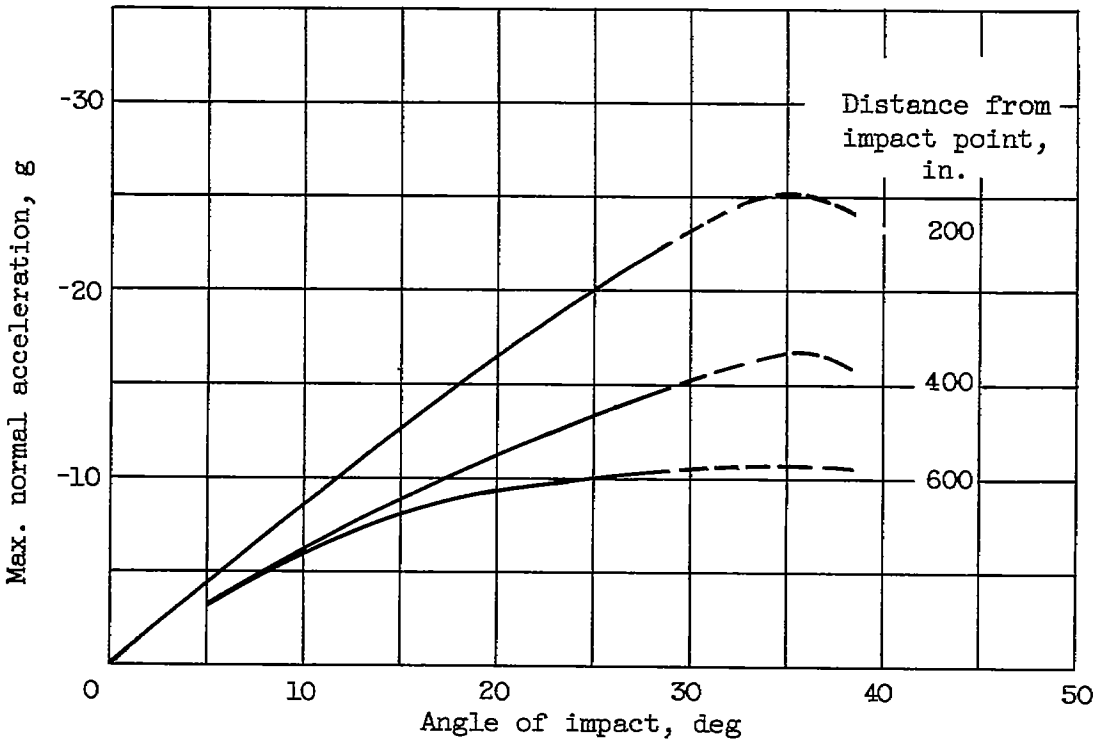

Figure 22. - Variation of maximum normal acceleration with impact angle during crashes of pressurized transports.

4462

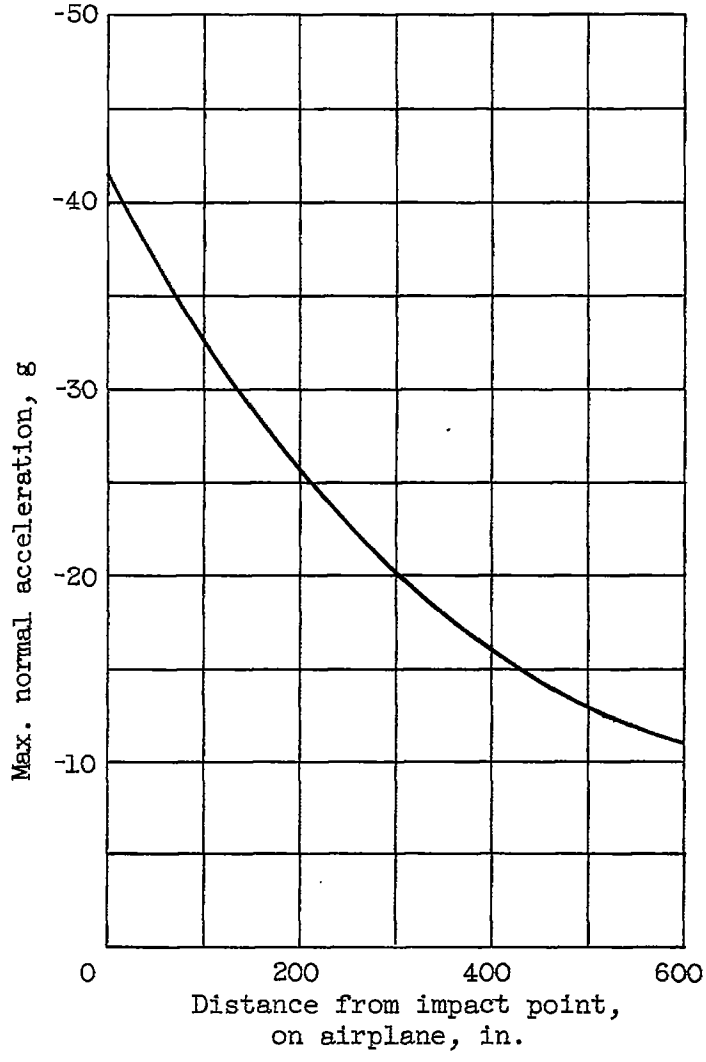

Figure 23. - Largest normal acceleration resulting from unflared landing crashes of pressurized transports at 35° impact angle (impact speed corrected to 95 mph).

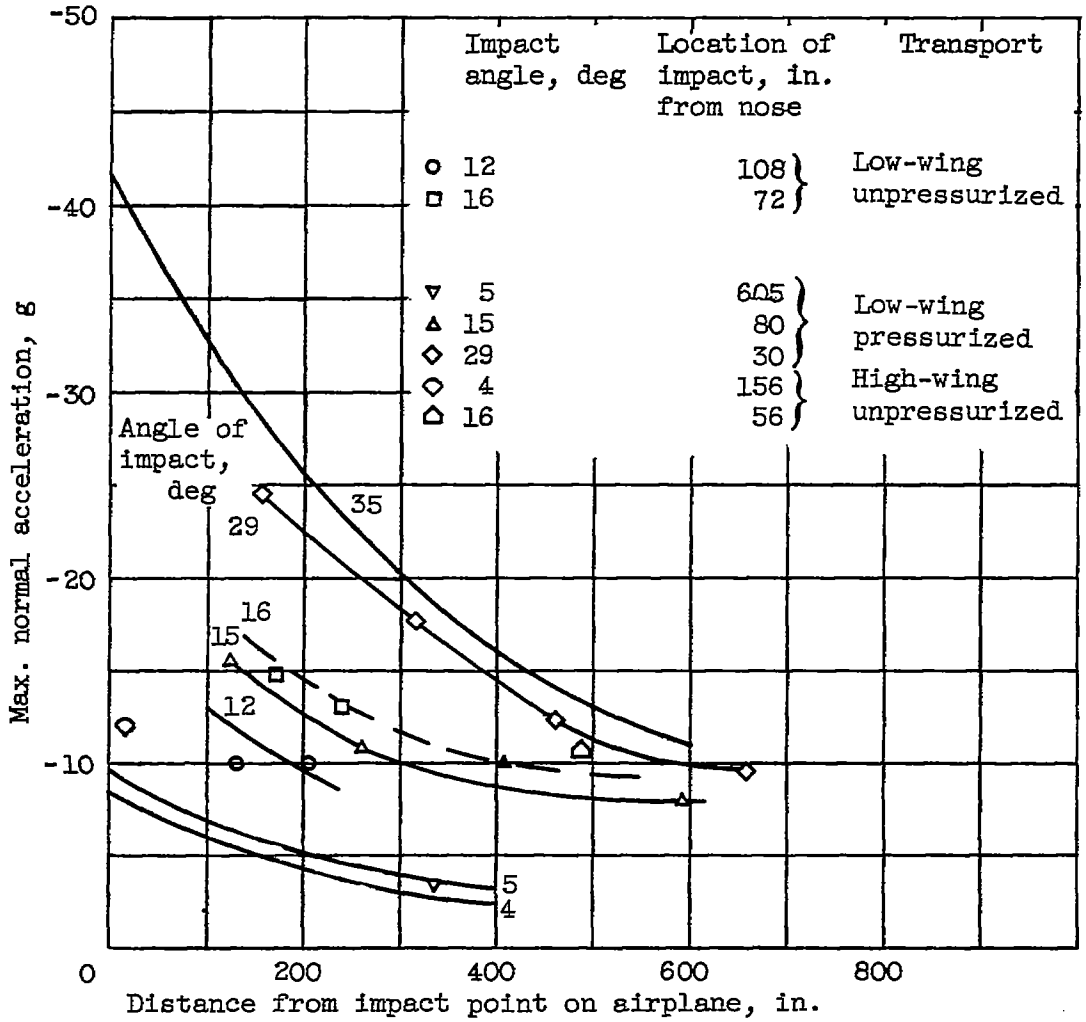

Figure 24. - Effect of position in airplane and airplane configuration on maximum normal accelerations during unflared landing crashes (impact velocity corrected to 95 mph).

F_{ns} = Force normal to inclined surface resulting from fuselage crumpling

F_{ps} = Force parallel to inclined surface resulting from friction and plowing of soil

i = Angle between inclined surface and airplane trajectory

s_c = Distance fuselage is crushed

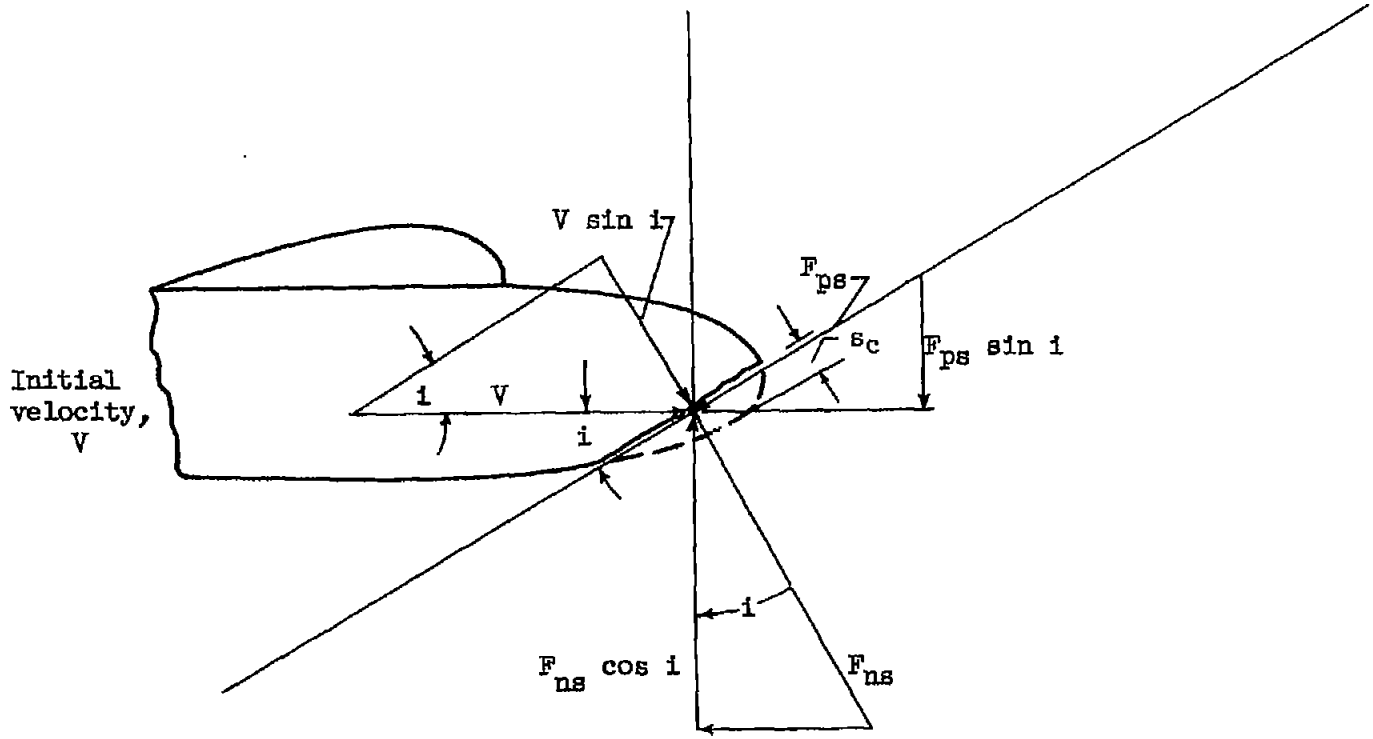

Figure 25. - Force and velocity diagram showing relation between (1) impact force normal to inclined surface that produces friction, compression, and plowing forces in a crash and (2) normal forces that change direction of airplane motion.

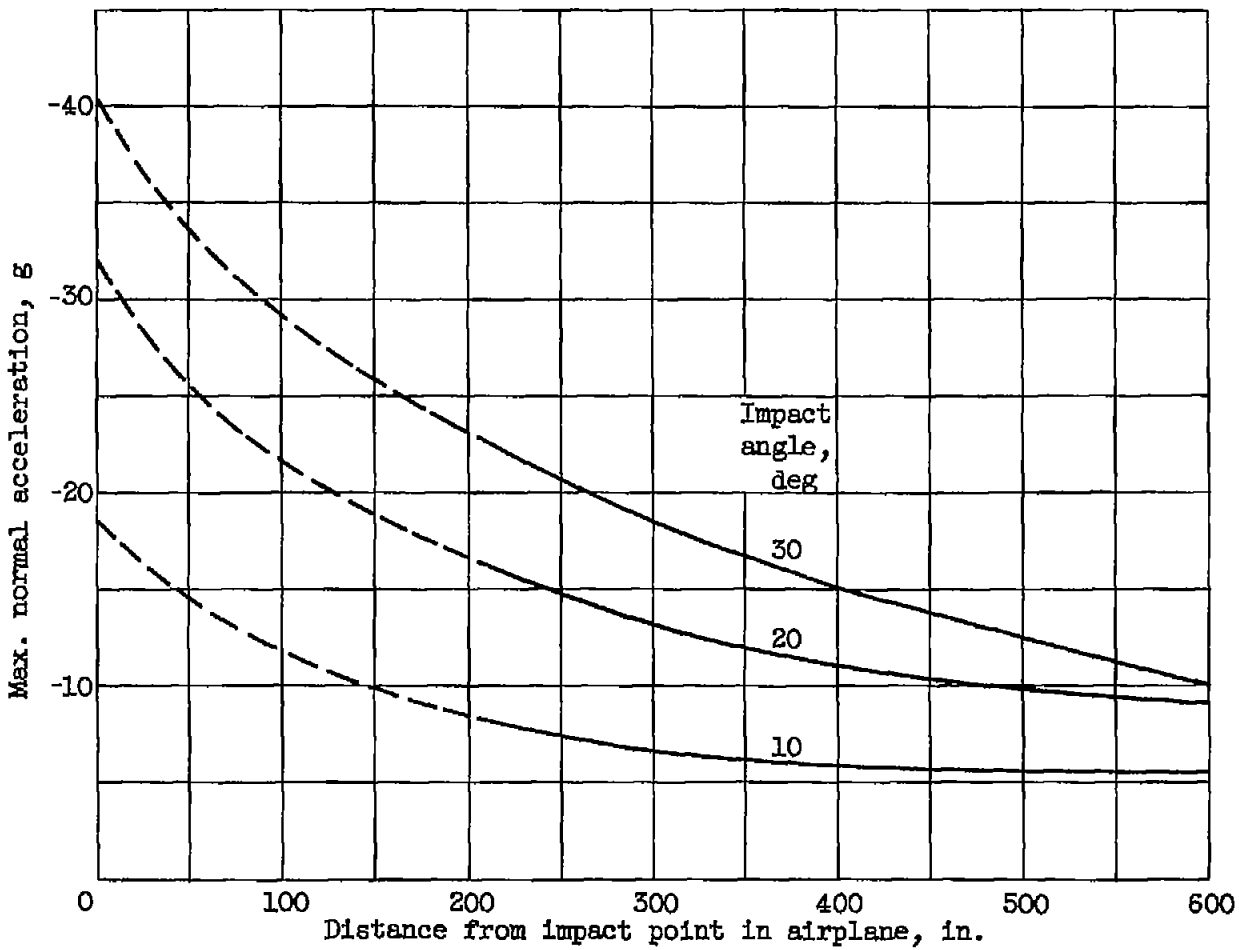

Figure 26. - Maximum normal acceleration in pressurized-transport airplane at various distances from impact point for impact angles of 10°, 20°, and 30° (impact speed corrected to 95 mph).

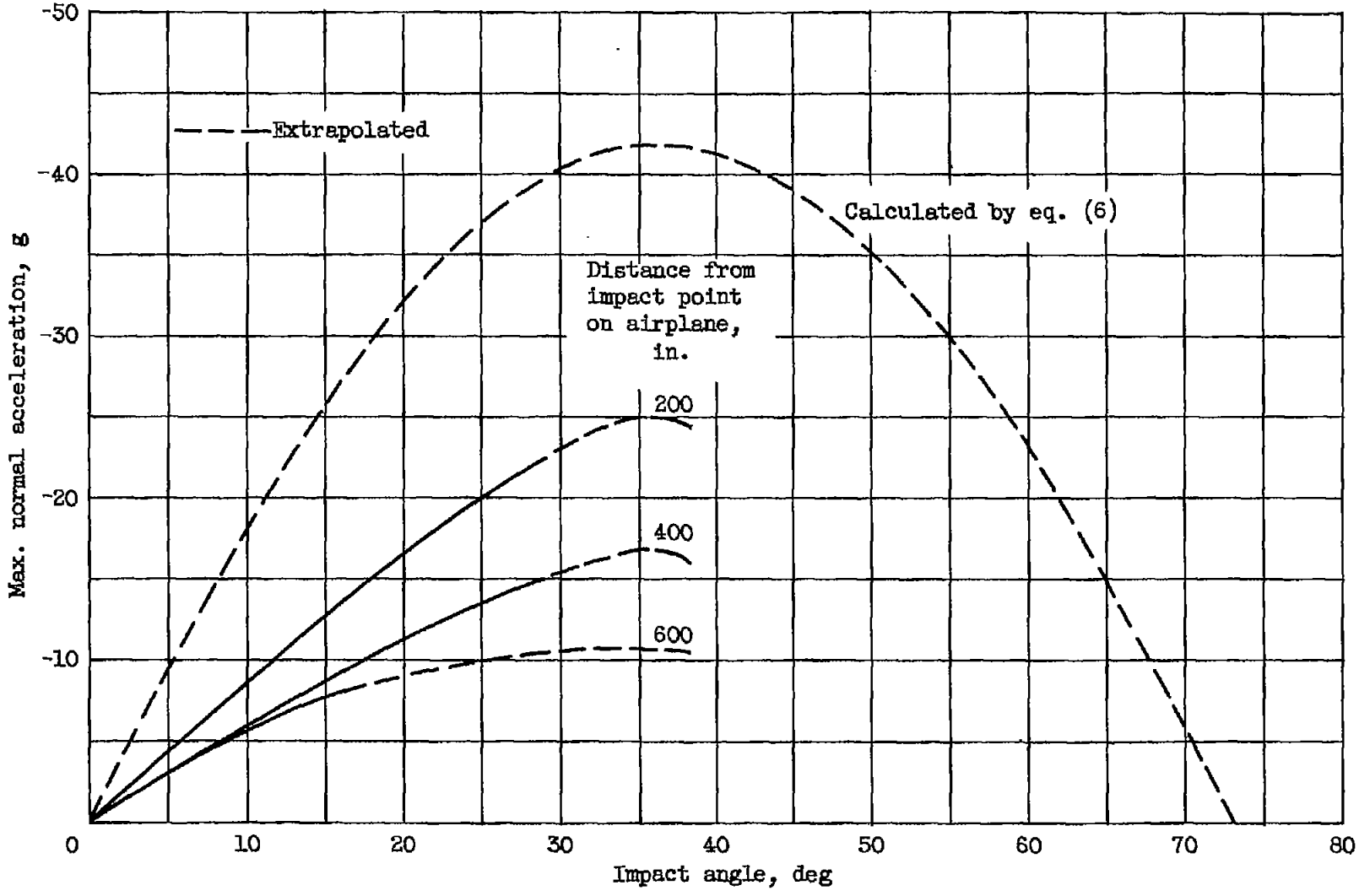

Figure 27. - Comparison of calculated and experimental values for maximum normal acceleration at various impact angles (impact speed corrected to 95 mph).

NACA - Langley Field, Va.